Appendix V
Runoff Block Evaporation, Infiltration and Routing

Evaporation

Evaporation is input for each month as parameter VAP (in subroutine RHYDRO) or as a time series in the Temp Block and used in equations in subroutine WSHED as parameter EVAP It is considered as a loss "off the top." That is, evaporation is subtracted from rainfall depths and/or ponded water prior to calculating infiltration. Thus, subsequent use of the symbol i for "rainfall intensity" is really rainfall intensity less evaporation rate. Although evaporation and infiltration are summed to form one total loss (RLOSS in subroutine WSHED) for the subcatchment runoff calculations, separate totals are maintained for the overall continuity check.

Infiltration

Introduction

For pervious areas SWMM users have the option of specifying one of two alternative infiltration models: the Horton model or the modified Green-Ampt model (Horton, 1940; Green and Ampt, 1911). Horton's model is empirical and is perhaps the best known of the infiltration equations. Many hydrologists have a "feel" for the best values of its three parameters despite the fact that little published information is available. In its usual form it is applicable only to events for which the rainfall intensity always exceeds the infiltration capacity, although the modified form used in SWMM is intended to overcome this deficiency.

On the other hand the Green-Ampt equation is a physically based model which can give a good description of the infiltration process. The Mein-Larson (1973) formulation of it is applicable also for the case of rainfall intensity being less than the infiltration capacity at the beginning of the storm. New data have been published to help users evaluate the parameter values (e.g., Carlisle et al., 1981). With results from these studies now being published, use of the Green-Ampt model for estimating infiltration should increase.

Integrated Horton's Equation

Cumulative Infiltration

SWMM and many other hydrologic analysis techniques have used Horton's equation (Horton, 1940) for prediction of infiltration capacity into the soil as a function of time,

$$f_p = f_\infty + (f_o - f_\infty)\, e^{-\alpha t} \qquad \text{(V-1)}$$

where

f_p	=	infiltration capacity into soil, ft/sec,
f_∞	=	minimum or ultimate value of f_p (at $t = \infty$), ft/sec,
f_o	=	maximum or initial value of f_p (at $t = 0$), ft/sec,
t	=	time from beginning of storm, sec, and
α	=	decay coefficient, sec^{-1}.

See Figure V-1 for a sketch of equation V-1. Actual infiltration is:

$$f(t) = \min [f_p(t), i(t)] \qquad \text{(V-2)}$$

where

f	=	actual infiltration into the soil, ft/sec, and
i	=	rainfall intensity, ft/sec.

Equation V-2 simply states that actual infiltration will be the lesser of actual rainfall and infiltration capacity.

Typical values for parameters f_o and f_∞ are often greater than typical rainfall intensities. Thus, when equation V-1 is used such that f_p is a function of time only, f_p will decrease even if rainfall intensities are very light, as sketched in Figure V-1. This results in a reduction in infiltration capacity regardless of the actual amount of entry of water into the soil.

To correct this problem, the integrated from of Horton's equation V-1 may be used:

$$F(t_p) = \int_0^{t_p} f_p \, dt = f_\infty \, t_p + \frac{(f_o - f_\infty)}{\alpha}\left(1 - e^{-\alpha t_p}\right) \qquad \text{(V-3)}$$

where F = cumulative infiltration at time t_p, ft.

This is shown schematically in Figure V-2 and assumes that actual infiltration has been equal to f_p. In fact, this is seldom the case, as sketched in Figure V-1. Thus, the true cumulative infiltration will be:

$$F(t) = \int_0^t f(\tau) d\tau \qquad \text{(V-4)}$$

where f is given by equation V-2.

Equations V-3 and V-4 may be used to define the time t_p. That is, actual cumulative infiltration given by equation V-4 is equated to the area under the Horton curve, given by equation V-3, and the resulting equation is solved for t_p and serves as its definition. Unfortunately, the equation:

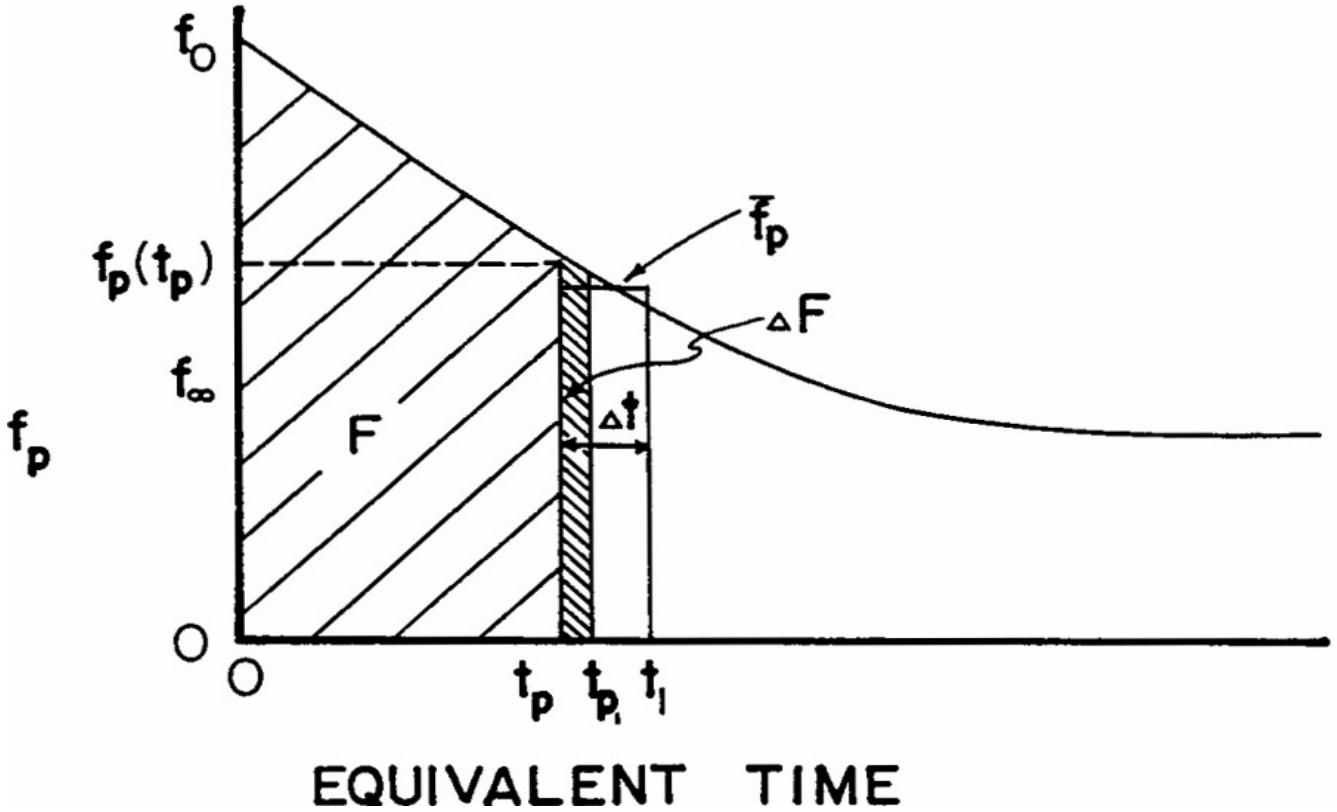

Figure V-1. Horton infiltration curve and typical hyetograph. For the case illustrated, runoff would be intermittent.

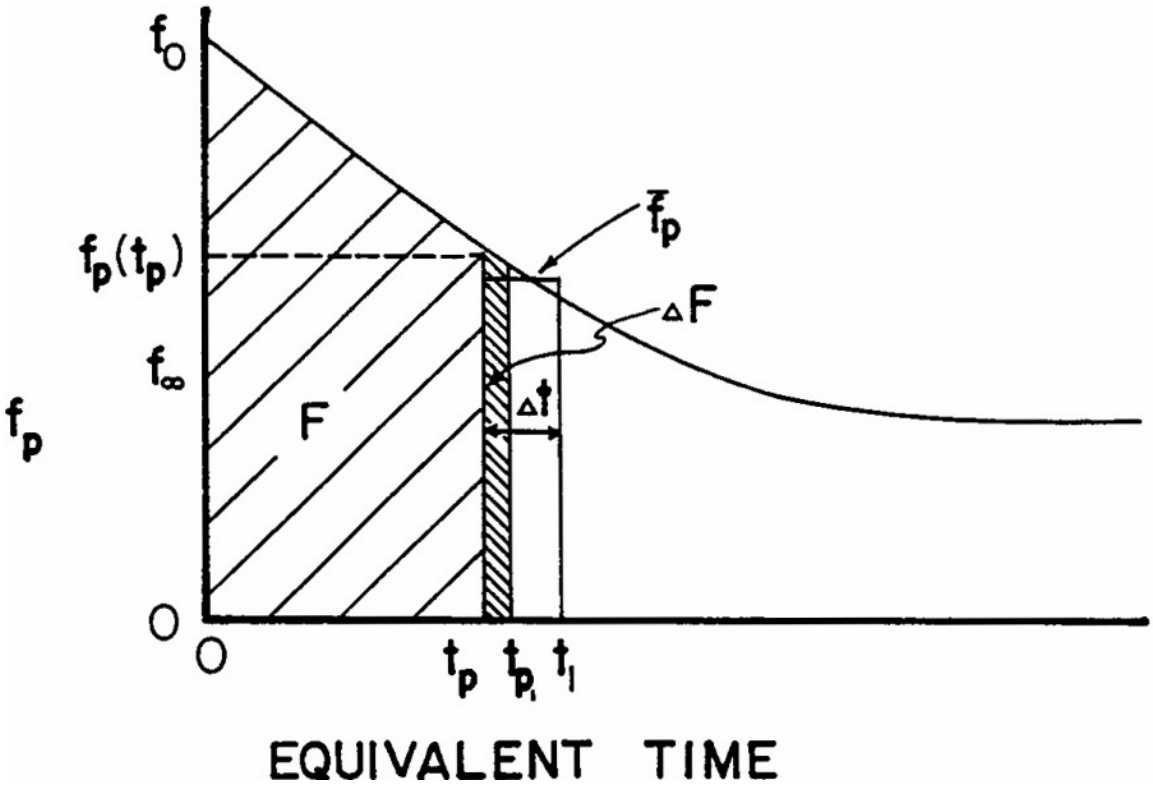

Figure V-2. Cumulative infiltration, F, is the integral of f, i.e., the area under the curve.

$$F = f_\infty t_p + \frac{(f_o - f_\infty)}{\alpha}\left(1 - e^{-\alpha t_p}\right) \qquad \text{(V-5)}$$

cannot be solved explicitly for t_p, and it must be done iteratively. Note that:

$$t_p \le t \qquad \text{(V-6)}$$

which states that the time t_p on the cumulative Horton curve will be less than or equal to actual elapsed time. This also implies that available infiltration capacity, $f_p(t_p)$ in Figure V-2, will be greater than or equal to that given by equation V-1. Thus, f_p will be a function of actual water infiltrated and not just a function of time that ignores other effects.

Summary of Procedure

Use of the cumulative Horton function in SWMM may be summarized as follows. Note that average values over time intervals are used.

1. At each time step, the value of f_p depends upon F, the actual infiltration up to that time. This is known by maintaining the value of t_p. Then the average infiltration capacity, f_p, available over the next time step is:

$$\bar{f}_p = \frac{1}{\Delta t}\int_{t_p}^{t_1 = t_p + \Delta t} f_p \, dt = \frac{F(t_1) - F(t_p)}{\Delta t} \qquad \text{(V-7)}$$

2. Equation V-2 is then used.

$$\bar{f} = \begin{cases} \bar{f}_p & \text{if} \quad \bar{i} \ge \bar{f}_p \\ \bar{i} & \text{if} \quad \bar{i} < \bar{f}_p \end{cases} \qquad \text{(V-8)}$$

where

$\bar{f}$ = average actual infiltration over the time step, ft/sec, and
$\bar{i}$ = average rainfall intensity over the time step, ft/sec.

3. Cumulative infiltration is then incremented.

$$F(t + \Delta t) = F(t) + \Delta F = F(t) + \bar{f}\,\Delta t \qquad \text{(V-9)}$$

where $\Delta F = \bar{f}\,\Delta t$ = additional cumulative infiltration, ft (see Figure R-5).

4. A new value of t_p is then found, t_{p_1}, from equation V-5. If $\Delta F = \bar{f}_p\,\Delta t$, t_{p_1} is found simply by $t_{p_1} = t_p + \Delta t$. However, it is necessary to solve equation V-5 iteratively when the new t_{p_1} will be less than $t_p + \Delta t$, as sketched in Figure V-2. This is done using the Newton-Raphson procedure:

$$FF = 0 = f_\infty t_p + \frac{(f_o - f_\infty)}{\alpha}\left(1 - e^{-\alpha t_p}\right) - F \qquad \text{(V-10)}$$

$$FF' = f_p(t_p) = f_\infty + (f_o - f_\infty)e^{-\alpha t_p} \qquad \text{(V-11)}$$

an initial guess is made for t_{p_1}, say

$$t_{p_1}(n) = t_p + \Delta t/2 \qquad \text{(V-12)}$$

where n refers to the number of the iteration. Then a correction is made to t_{p_1} using FF and FF′,

$$t_{p_1}(n+1) = t_{p_1}(n) - FF/FF' \qquad \text{(V-13)}$$

The convergence criterion is:

$$FF/FF' < 0.001\ \Delta t \qquad \text{(V-14)}$$

and is achieved quite rapidly.

5. If $t_p \geq 16/\alpha$, the Horton curve is essentially flat and $f_p = f_\infty$. Beyond this point there is no need to iterate since f_p will be constant at f_∞ and independent of F.

Regeneration of Infiltration Capacity

For continuous simulation, infiltration capacity will be regenerated (recovered) during dry weather. SWMM performs this function whenever there are dry time steps - no precipitation or surface water - according to the hypothetical drying curve sketched in Figure V-3.

$$f_p = f_o - (f_o - f_\infty)e^{-\alpha_d (t - t_w)} \qquad \text{(V-15)}$$

where

α_d = decay coefficient for the recovery curve, sec^{-1}, and
t_w = hypothetical projected time at which $f_p = f_\infty$ on the recovery curve, sec.

In the absence of better knowledge of α_d, it is taken to be a constant fraction or multiple of α:

$$\alpha_d = R\,\alpha \qquad \text{(V-16)}$$

where R = constant ratio, probably ≥ 1.0 (implying a "longer" drying curve than wetting curve).

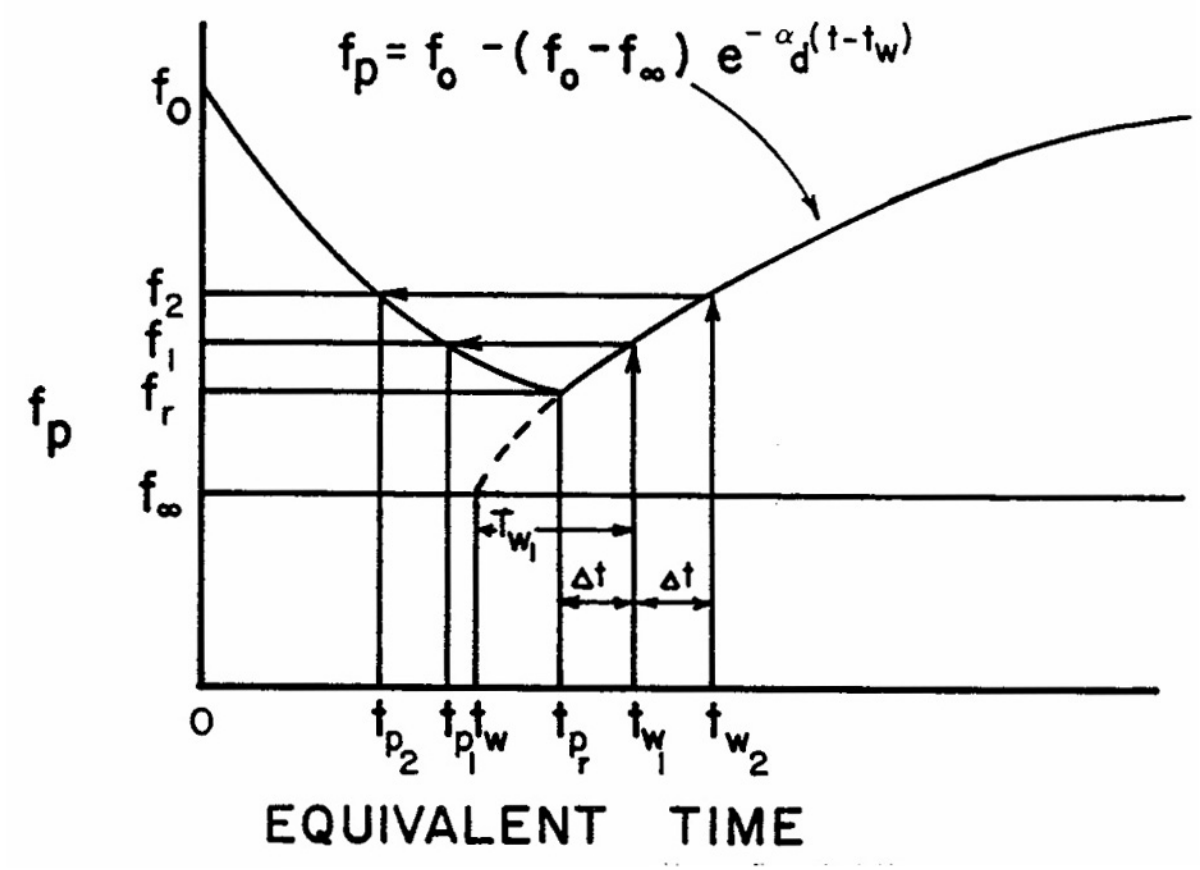

Figure V-3. Regeneration (recovery) of infiltration capacity during dry time steps.

New values of t_p are then generated as indicated in Figure V-3. Let

t_{p_r} = value of t_p at beginning of recovery, sec,
f_r = corresponding value of f_p, ft/sec, and
T_{w_1} = $t_{w_1} - t_w$, $T_{w_2} = t_{w_2} - t_w$, etc.

Thus, along the recovery curve, for example,

$$f_1 = f_p\left(t_{w_1}\right) = f_o - \left(f_o - f_\infty\right) e^{-\alpha_d T_{w_1}} \qquad \text{(V-17)}$$

Solving equation V-17 for the initial time difference, T_{w_r},

$$T_{w_r} = t_{p_r} - t_w = \frac{1}{\alpha_d} \ln \frac{f_o - f_\infty}{f_o - f_r} \tag{V-18}$$

Then

$$T_{w_1} = T_{w_r} + \Delta t \tag{V-19}$$

and f_1 in Figure V-3 is found from equation V-17. Finally t_{p_1} is found from equation V-1,

$$t_{p_1} = \frac{1}{\alpha} \ln \frac{f_o - f_\infty}{f_1 - f_\infty} \tag{V-20}$$

The procedure may be summarized as follows:

1. Knowing t_{p_r}, find f_r from equation V-1.
2. Solve for T_{w_r} from equation V-18.
3. Increment T_{w_r} according to equation V-19.
4. Solve for f_1 from equation V-17.
5. Solve for t_{p_1} from equation V-20.

All steps are combined in:

$$t_{p_1} = -\frac{1}{\alpha} \ln \left[1 - e^{-\alpha_d \Delta t} \left(1 - e^{-\alpha t_{p_r}} \right) \right] \tag{V-21}$$

On succeeding time steps, t_{p_1} may be substituted for t_{p_r} and t_{p_2} may be substituted for t_{p_1}, etc. Note that f_p has reached its maximum value of f_o when $t_p = 0$.

Program Variables

The infiltration computations are performed in subroutine WSHED in the Runoff Module of SWMM. Correspondence of program variables to those of this subsection is as follows:

Δt	=	DELT	t_{p_1}	=	TP1
f_o	=	WLMAX	FF	=	FF
f_∞	=	WLMIN	FF′	=	DFF
α	=	DECAY	$\bar{f}$	=	RLOSS (RLOSS is also the sum of
R	=	REGEN			infiltration plus evaporation)
t_p	=	TP	$\bar{i}$	=	RI
F	=	CUMINF = CUMI	$\bar{f}_p$	=	RLOSS1

Green-Ampt Equation

Infiltration During Rainfall Events

The Green-Ampt equation (Green and Ampt, 1911) has received considerable attention in recent years. The original equation was for infiltration with excess water at the surface at all times. Mein and Larson (1973) showed how it could be adapted to a steady rainfall input and proposed a way in which the capillary suction parameter could be determined. More recently Chu (1978) has shown the applicability of the equation to the unsteady rainfall situation, using data for a field catchment.

The Mein-Larson formulation is a two-stage model. The first step predicts the volume of water which will infiltrate before the surface becomes saturated. From this point onward, infiltration capacity is predicted by the Green-Ampt equation. Thus:

For $F < F_s$:

$$F_s = \frac{S \cdot IMD}{i/K_s - 1} \quad \text{for } I > K_s$$

$$f = i \quad \text{and} \quad \text{No calculation of } f_s \text{ for } i \le K_s \tag{V-22}$$

For $F \ge F_s$:

$$f = f_p \quad \text{and} \quad f_p = K_s\left(1 + \frac{S \cdot IMD}{F}\right) \tag{V-23}$$

where

f	=	infiltration rate, ft/sec,
f_p	=	infiltration capacity, ft/sec,
i	=	rainfall intensity, ft/sec,
F	=	cumulative infiltration volume, this event, ft,
F_s	=	cumulative infiltration volume required to cause surface saturation, ft,
S	=	average capillary suction at the wetting front, ft water,
IMD	=	initial moisture deficit for this event, ft/ft, and
K_s	=	saturated hydraulic conductivity of soil, ft/sec.

Equation V-22 shows that the volume of rainfall required to saturate the surface depends on the current value of the rainfall intensity. Hence, at each time step for which $i > K_s$, the value of f_s is calculated and compared with the volume of rainfall already infiltrated for this event. Only if $F \ge F_s$ does the surface saturate, and further calculations for this condition use equation V-23.

When rainfall occurs at an intensity less than or equal to K_s, all rainfall infiltrates and is used only to update the initial moisture deficit, IMD. (The mechanism for this is discussed in the next subsection with reference to equation V-31.) The cumulative infiltration is not altered for this case of low rainfall intensity (relative to the saturated hydraulic conductivity, K_s).

Equation V-23 shows that the infiltration capacity after surface saturation depends on the infiltrated volume, which in turn depends on the infiltration rates in previous time steps. To avoid numerical errors over long time steps, the integrated form of the Green-Ampt equation is more suitable. That is, f_p is replaced by dF/dt and integrated to obtain:

$$K_s(t_2 - t_1) = F_2 - C \diamond \ln(F_2 + C) - F_1 + C \diamond \ln(F_1 + C) \quad \text{(V-24)}$$

where

C	=	IMD ◈ S, ft of water,
t	=	time, sec, and
1,2	=	subscripts for start and end of time interval respectively.

Equation V-24 must be solved iteratively for F_2, the cumulative infiltration at the end of the time step. A Newton-Raphson routine is used.

The infiltration volume during time step $(t_2 - t_1)$ is thus $(t_2 - t_1) \diamond i$ if the surface does not saturate and $(F_2 - F_1)$ if saturation has previously occurred and a sufficient water supply is at the surface. If saturation occurs during the time interval, the infiltration volumes over each stage of the process within the time steps are calculated and summed. When rainfall ends (or falls below infiltration capacity) any water ponded on the surface is allowed to infiltrate and added to the cumulative infiltration volume.

Recovery of Infiltration Capacity (Redistribution)

Evaporation, subsurface drainage, and moisture redistribution between rainfall events decrease the soil moisture content in the upper soil zone and increase the infiltration capacity of the soil. The processes involved are complex and depend on many factors. In SWMM a simple empirical routine is used as outlined below; commonly used units are given in the equations to make the description easier to understand.

Infiltration is usually dominated by conditions in the uppermost layer of the soil. The thickness of this layer depends on the soil type; for a sandy soil it could be several inches, for a heavy clay it would be less. The equation used to determine the thickness of the layer is:

$$L = 4 \cdot \sqrt{K_s} \quad \text{(V-25)}$$

where:

L	=	thickness of layer, in., and
K_s	=	saturated hydraulic conductivity, in./hr.

Thus for a high K_s of 0.5 in,/hr (12.7 mm/hr) the thickness computed by equation V-25 is 2.83 inches (71.8 mm). For a soil with a low hydraulic conductivity, say K_s = 0.1 in./hr (2.5 mm/hr), the computed thickness is 1.26 inches (32.1 mm).

A depletion factor is applied to the soil moisture during all time steps for which there is no infiltration from rainfall or depression storage. This factor is indirectly related again to the saturated hydraulic conductivity of the soil and is calculated by:

$$DF = L/300 \quad \text{(V-26)}$$

where

DF = depletion factor, hr^{-1}, and
L = depth of upper zone, in.

Hence, for K_s = 0.5 in./hr (12.7 mm/hr), DF = 0.9 percent per hour; for K_s = 0.1 in./hr (2.5 mm/hr), DF = 0.4 percent per hour. The depletion volume (DV) per time step is then:

$$DV = DF \diamond FU_{max} \diamond \Delta t \quad \text{(V-27)}$$

where

FU_{max} = $L \diamond IMD_{max}$ = saturated moisture content of the upper zone, in.,
IDM_{max} = maximum initial moisture deficit, in./in., and
Δt = time step, hr.

The computations used are:

$$FU = FU - DV \quad \text{for} \quad FU \geq 0 \quad \text{(V-28)}$$

$$F = F - DV \quad \text{for} \quad F \geq 0 \quad \text{(V-29)}$$

where

FU = current moisture content of upper zone, in., and
F = cumulative infiltration volume for this event, in.

To use the Green-Ampt infiltration model in continuous SWMM, it is necessary to choose a time interval after which further rainfall will be considered as an independent event. This time is computed as:

$$T = 6/(100 \diamond DF) \quad \text{(V-30)}$$

where T = time interval for independent event, hr.

For example, when K_s = 0.5 in./hr (12.7 mm/hr) the time between independent events as given in the equation V-30 is 6.4 hr; when K_s = 0.1 in./hr (2.5 mm/hr) the time is 14.3 hr. After time T has elapsed the variable F is set to zero, ready for the next event. The moisture remaining in the upper zone of the soil is then redistributed (diminished) at each time step by equation V-28 in order to update the current moisture deficit (IMD). The deficit is allowed to increase up to its maximum value (IMD_{max}, an input parameter) over prolonged dry periods. The equation used is

$$IMD = \frac{F_{max} - FU}{L} \qquad \text{for } IMD \le IMD_{max} \tag{V-31}$$

When light rainfall ($i \le K_s$) occurs during the redistribution period, the upper zone moisture storage, FU, is increased by the infiltrated rainfall volume and IMD is again updated using equation V-31.

Guidelines for estimating parameter values for the Green-Ampt model are given in Section 4. As is also the case for the Horton equation, different soil types can be modeled for different subcatchments.

Program Variables

The infiltration computations are performed in subroutines WSHED and GAMP in the RUNOFF Block. Correspondence of program variables to those of this subsection is as follows:

S	=	SUCT(J)	L	=	UL(J)
IMD_{max}	=	SMDMAX (J)	DF	=	DF(J)
K_s	=	HYDCON(J)	i	=	RI
FU_{max}	=	FUMAX(J)	t	=	time
FU	=	FU(J)	Δt	=	DELT
IMD	=	SMD(J)	DV	=	DEP
F	=	F(J)	F_s	=	FS

Subcatchment Runoff Calculations

Overland Flow

The RUNOFF Block forms the origin of flow generation within SWMM, and much of the emphasis in data preparation and user effort is aimed at successful execution of this block. In order to understand better the conversion of rainfall excess (rainfall and/or snowmelt less infiltration and/or evaporation) into runoff (overland flow), this subsection briefly describes the equations used for this purpose. It is intended to supplement the material presented in the original SWMM documentation (Metcalf and Eddy et al., 1971a).

As discussed in Section 4, subcatchments are subdivided into three subareas that simulate impervious areas, with and without depression (detention) storage, and pervious area (with depression storage). These are areas A1, A3, and A2 respectively on Figure V-4 and are denoted in subroutine WSHED by the subscript J, (J = 1, 2, 3, 4). When snowmelt is included, a fourth subarea is added to account for the presence or absence of snow cover (see Figure II-5 in Appendix II), but that case will not be considered further here. The depth of depression storage is an input parameter (WSTORE) for the impervious and pervious areas of each catchment. The impervious area without depression storage is specified for all subcatchments by parameter PCTZER (as a percent),

$$A3 = \frac{PCTZER}{100} \cdot (A1 + A3) \tag{V-32}$$

Of course, any subcatchment may be assigned zero depression storage over its entirety through the use of parameter WSTORE.

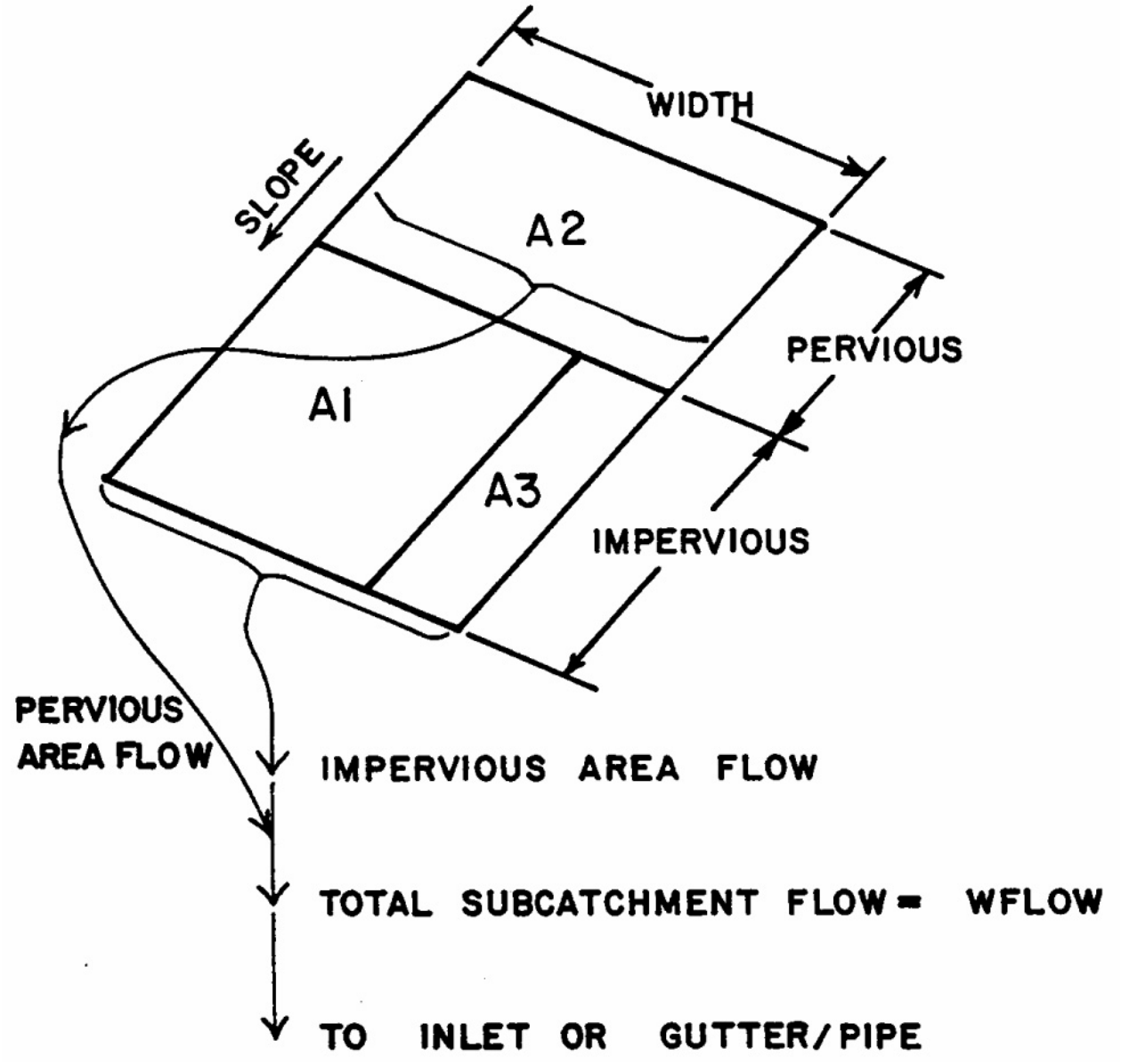

Figure V-4. Subcatchment schematization for overland flow calculations. Flow from each subarea is directly to an inlet or gutter/pipe. Flow from one subarea is not routed over another subarea.

Overland flow is generated from each of the three subareas by approximating them as non-linear reservoirs, as sketched in Figure V-5. This is a spatially "lumped" configuration and really assumes no special shape. However, if the subcatchment width, W, is assumed to represent a true prototype width of overland flow, then the reservoir will behave as a rectangular catchment, as sketched in Figure V-4. Otherwise, the width (and the slope and roughness) may be considered calibration parameters and used to adjust predicted to measured hydrographs.

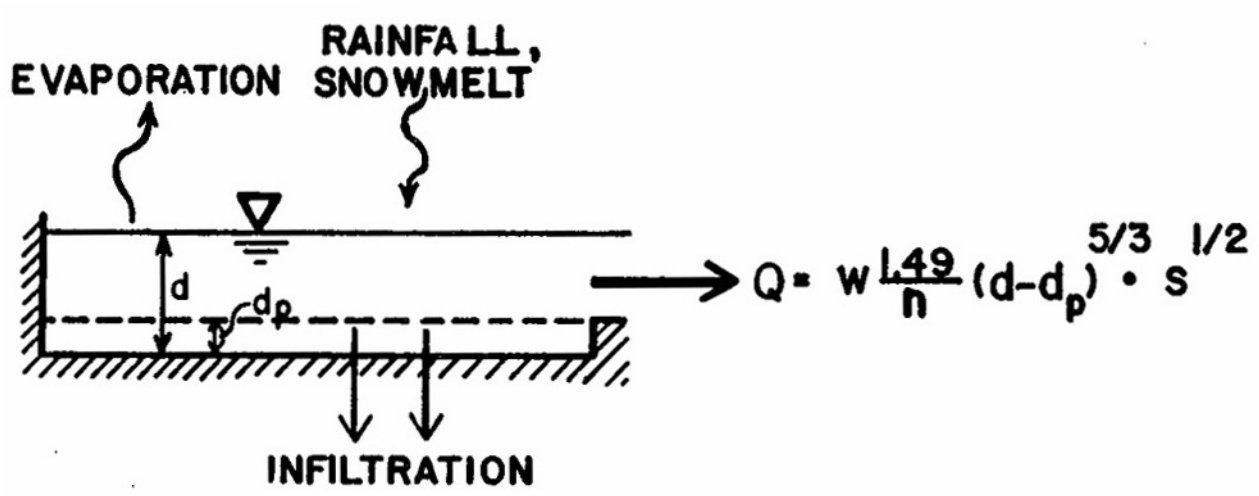

Figure V-5. Non-linear reservoir model of subcatchment.

The non-linear reservoir is established by coupling the continuity equation with Manning's equation. Continuity may be written for a subarea as

$$\frac{dV}{dt} = A\frac{dd}{dt} = A \cdot i^* - Q \qquad \text{(V-33)}$$

where

V	=	A ◈ d = volume of water on the subarea, ft^3,
d	=	water depth, ft,
t	=	time, sec,
A	=	surface area of subarea, ft^2,
i*	=	rainfall excess = rainfall/snowmelt intensity minus evaporation/infiltration rate, ft/sec, and
Q	=	outflow rate, cfs.

The outflow is generated using Manning's equation:

$$Q = W \cdot \frac{1.49}{n}\left(d - d_p\right)^{5/3} S^{1/2} \tag{V-34}$$

where

W	=	subcatchment width, ft,
n	=	Manning's roughness coefficient,
d_p	=	depth of depression storage, ft, and
S	=	subcatchment slope, ft/ft.

Equations V-33 and V-34 may be combined into one non-linear differential equation that may be solved for one unknown, the depth, d. This produces the non-linear reservoir equation:

$$\begin{aligned} \frac{dd}{dt} &= i^* - \frac{1.49 \cdot W}{A \cdot n}\left(d - d_p\right)^{5/3} S^{1/2} \\ &= i^* + WCON \cdot \left(d - d_p\right)^{5/3} \end{aligned} \tag{V-35}$$

where

$$WCON = -\frac{1.49 \cdot W \cdot S^{1/2}}{A \cdot n} \tag{V-36}$$

Note the grouping of width, slope and roughness into only one parameter.

Equation V-35 is solved at each time step by means of a simple finite difference scheme. For this purpose, the net inflow and outflow on the right hand side (RHS) of the equation must be averaged over the time step. The rainfall excess, i*, is given in the program as a time step average. The average outflow is approximated by computing it using the average between the old and new depths. That is, letting subscripts 1 and 2 denote the beginning and the end of a time step, respectively, equation V-35 is approximated by:

$$\frac{d_2 - d_1}{\Delta t} = i^* + WCON \cdot \left[d_1 + \frac{1}{2}\left(d_2 - d_1\right) - d_p\right]^{5/3} \tag{A-37}$$

where Δt = time step, sec.

Equation V-37 is then solved for d_2 using a Newton-Raphson iteration; the Fortran coding is located near the end of subroutine WSHED.

Given d_2, the instantaneous outflow at the end of a time step, WFLOW is computed using the equation V-34. Parameter WFLOW is used in runoff quality calculations and is the flow

value that is input to inlets and gutter/pipes. The instantaneous outflow at a given time is also the flow value transferred to subsequent SWMM modules.

Although the solution of equation V-37 is straightforward and simple (and in fact may be performed on programmable hand calculators), some peculiarities exist in the way the parameters for individual subareas (A1, A2, A3 in Figure V-4) are specified. In particular, only two values of WCON are computed (equation V-36), one for the pervious and one for the total impervious subareas. Thus, WCON is the same for calculating depths on subareas A1 and A3 and is computed from equation V-36 using the total impervious area, A1 plus A3, in the denominator. However, the instantaneous flow is computed using the individual area of each subarea (e.g., Al or A3). The net effect for subareas A1 and A3 is approximately to reduce the subcatchment width by the ratio A1/(A1 + A3) or A3/(A1 + A3) as implied in Figure V-4. Numerical tests of this scheme versus one that uses the individual areas (and proportional widths) in parameter WCON indicate only about a half percent difference between the two methods. Hence, it should be satisfactory.

Prior to performing these calculations, a check is made to see if losses are greater than the rainfall depth plus ponded water. If so, the losses (evaporation plus infiltration) absorb all water and outflow is zero. Similarly, if losses alone would be sufficient to lower the depth below the depression storage, the new depth is computed on this basis only and the outflow is zero.

The computational scheme (equations V-37 and V-38) has proven quite stable. The only instance for which non-convergence problems arise (or an attempt to compute a negative depth) is when the subarea values are very small (e.g., a few square feet) coupled with a large time step (e.g., ten minutes). Should a non-convergence message be printed, the problem may usually be cured by increasing the appropriate area or decreasing the time step.

Channels and Pipes

Flow routing in channel/pipes is also performed by coupling the continuity equation with Manning's equation to produce a non-linear reservoir. The solution technique is performed in subroutine GUTNR and is entirely analogous to that just described for overland flow; no details will be given here. However, a few comments are in order. Three cross sectional shapes are available for channel/pipes: circular, trapezoidal, and parabolic. Trapezoidal channels and circular pipes are shown in Figure V-6 (parabolic channels are shown in Figure 4-9). Parameters representing depth (e.g., GDEPTH, D1, D0) are actual depths, in feet, for trapezoidal channels but not for circular pipes. Rather, for pipes the "depth" parameters are half of the angle subtended by the wetted perimeter, in radians, as shown in Figure V-6. Knowledge of this fact aids in understanding the Fortran coding in subroutine GUTTER.

Since a channel/pipe acts as a reservoir with a water surface parallel to the invert, inflows are automatically "distributed" along its length. Hence, concentration of subcatchment inflows only at the upstream end of a channel/pipe may be reasonable. On the other hand, this leads to considerable dispersion or flattening of a hydrograph peak when it is routed through a cascade of channel/pipes. Of course, for this flow routing scheme, downstream changes are not "felt" upstream, and no backwater effects can be simulated.

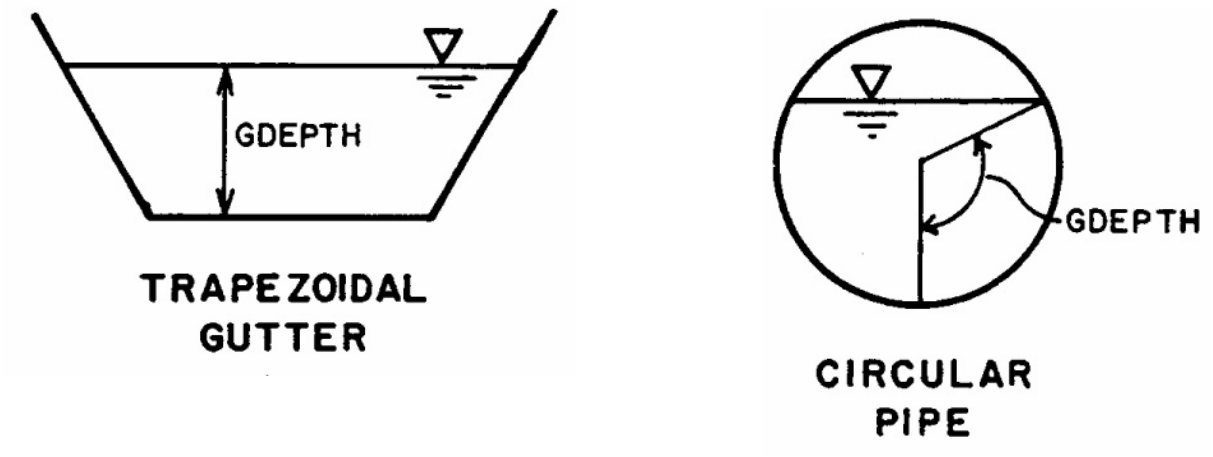

Figure V-6. Depth parameters for trapezoidal channel and circular pipe.

Non-convergence messages may be encountered during channel/pipe routing if short channel/pipes of small dimensions are included in the simulation. Again, this can usually be cured by increasing the dimensions (e.g., length and width/diameter) or decreasing the time step. The iterative equation for the Newton-Raphson technique used to solve for the new depth in the channel/pipe has been adjusted to eliminate most convergence problems. This new iterative equation plus the method used for variable time steps in Runoff will let the user have reasonably sized pipes in his/her simulation even for long time steps.

Variable Time Step

Runoff has three time steps: (1) a wet time step (WET), (2) the transitional time step(s) between wet and dry (WETDRY), and (3) the dry (DRY) time step. WET will normally be less than or equal to the rainfall interval entered on data group D1. It can be longer, but information is lost by averaging the rainfall over a longer time period. A wet time step is a time step with precipitation occurring on <u>any</u> subcatchment. A transitional time step has no precipitation input on any subcatchment, but the subcatchment(s) still have water remaining in surface storage. A dry time step has no precipitation input or surface storage. However, it can have groundwater flow. The model is considered either globally wet, globally transitional, or globally dry.

The time step should be smaller for periods of rapid change, i.e., during rainfall, and longer during periods of slower change, i.e., during transitional and dry time steps. Runoff by using the concept of extrapolation to the limit can use any time step from 1 second to 1 year. The solution technique is stable and convergent for any length time step.

Typically the WET time step should be a fraction of the rainfall interval. Five minute rainfall should have wet time steps of 1, 2.5 or 5.0 minutes, for example. The rainfall intensity is constant over the wet time step when WET is a fraction of the rainfall interval. A smaller wet time step would be desirable when the subcatchment is small and the time of concentration is a fraction of the rainfall interval. When using one-hour rainfall from the NWS, wet time steps of 10 minutes, 15 minutes, etc., can be used by the model.

The Runoff overland flow routing technique loses water through infiltration, evaporation, and surface water outflow during the transition periods. A subcatchment's surface storage and surface flow always decrease during the transition from a wet condition to a dry condition. A smooth curve or straight line is a good model for the shape of the hydrograph. Transport and Extran usually have small time steps and use linear or parabolic interpolation for input hydrographs with longer time steps. The transition time step, WETDRY, can be substantially longer than WET and generate a good overland flow hydrograph. For example, a WET of 5 minutes can be coupled with a WETDRY of 15 minutes or 30 minutes. When using hourly rainfall input, a WET of 15 minutes can be coupled to a WETDRY of 2 hours or 3 hours.

The dry time step should be one day to a week. The dry time step is used to update the infiltration parameters, generate groundwater flow, and produce a time step value for the interface file. The dry time step should be day(s) in wet climates and days or week(s) in very dry climates. The synoptic analysis performed by the Rain Block will be of use in selecting the appropriate dry time step. Examine the average storm interevent duration in the storm summary table. The average storm interevent duration ranges from half a week to months depending on station location.

The model can achieve substantial time savings with judicious usage of WET, DRY, and WETDRY for both short and long simulations. As an example consider the time step saving using a WET of 15 minutes, a WETDRY of 2 hours, and a DRY of 1 day versus using a single time step of 1 hour for a year. Using Florida rainfall as input (average annual rainfall between 50 and 60 inches) gives 300 wet hours per year, flow for approximately 60 days per year, and 205 dry days per year. This translates to 1975 time steps. A constant hourly time step for one year requires 8760 time steps. This is greater than a 400 percent savings in time with a better representation of the flow hydrograph due to the 15 minute wet time step.

Extrapolation Technique

The accuracy of the solution technique using variable time steps is enhanced (aided) by a numerical technique called Richardson extrapolation (Press et al., 1986). Richardson extrapolation is also called Richardson's deferred approach to the limit. The extrapolated value is the solution that would be obtained if an infinitely small time step was used in watershed, channel/pipe or infiltration routing.

The concept of extrapolation to the limit may be more familiar to the reader in connection with Romberg integration. Romberg integration repeatedly calls a trapezoidal rule integration subroutine in the sequence 1, 2, 4, 8, 16 panels etc. to extrapolate a more accurate solution than that obtained by the trapezoidal rule alone.

The Runoff Block uses the same concept to extrapolate the watershed depth at the end of a time step. The subroutine WSHED uses the iterative techniques described earlier in this appendix to solve for the infiltration volume and watershed depth at the end of a time step. The WET, DRY, and WETDRY time steps are broken up into smaller and smaller steps using the relationships: WET/n, DRY/n, and WETDRY/n where n is the number of subintervals used by WSHED. The sequence of subintervals n used by WSHED is

n = 1,2,4,6,8,12,24,32,48,64

Experience has shown that time steps smaller than 5 minutes do not have to be broken into subintervals. The integrated depth or infiltration volume for one subinterval is almost equal

to the extrapolated depth or infiltration volume obtained from using more subintervals. For time steps longer than 5 minutes the extrapolated answer obtained from using one and two subintervals usually has a small estimated error. The exceptions are due to large rainfall intensities over long time periods (i.e., 15 minute to 1 hour rainfall). It may be necessary for the time step to be broken up into more than 32 subintervals during these conditions.

The extrapolation to an infinitely small time step is illustrated in Figure V-7. A rational function, which is a analytical function dependent on the step size h, is fit to the various estimates of the integrated watershed depth or infiltration volume. The rational function (a function with polynomial numerator and denominator) is then evaluated at h = 0. The evaluated depth or volume is the extrapolated value.

The Runoff Block treats overland flow, infiltration, and groundwater flow as coupled processes. The extrapolated value is actually a vector of estimates. This is in contrast to SWMM 3 where the infiltration and overland flow were not coupled.

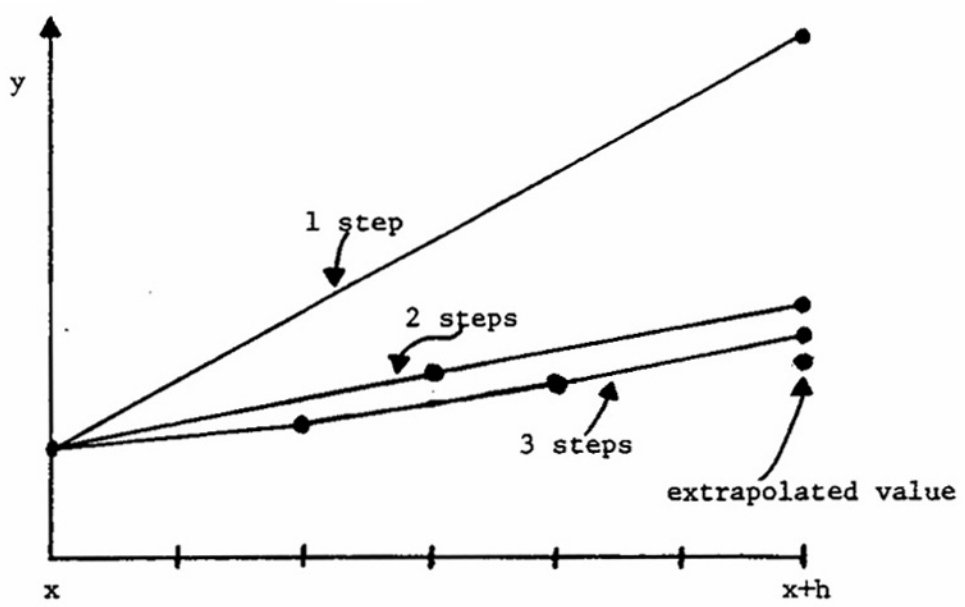

Figure V-7. Richardson extrapolation as used in the Runoff Block. A large interval is spanned by different sequences of finer and finer substeps. Their results are extrapolated to an answer that corresponds to an infinitely small time step. Runoff uses a Newton-Raphson iteration solution for the y values at each time step, and a rational function extrapolation to calculate the extrapolated y value. (This graph is adapted from Press et al., 1986.)

Appendix VI
Transport Block Scour and Deposition

Introduction

Deposition of solid material during dry-weather flow (DWF) in combined sewers and subsequent scour during wet-weather flow has long been assumed to form a significant contribution of solids to combined sewer overflows. The deposition-scour phenomenon is also evident in the "first flush" – high solids concentrations at the beginning of a storm event – found in many sewer systems. Even storm sewer systems may show a first flush if there is a base flow due to infiltration or illegal connections.

Deposition and scour processes were included in the original SWMM Transport Block as described in the documentation (Metcalf and Eddy et al., 1971a). It simulated solids buildup during DWDAYS dry days prior to the storm and scour during the storm, as velocities increased. A constant horizontal approximation to the dimensionless shear stress on Shield's curve (described subsequently) was used to determine incipient motion, and one fixed particle size distribution (for suspended solids only) and specific gravity of 2.7 were used to characterize the solids.

Several problems existed in the routine, perhaps unknown to most SWMM users. The deposition-scour was dependent on the time step. Buildup of solids would occur using a 1-hr time step for the dry days prior to simulation, but scour would occur using, say, a 10-min simulation time step with the same flow conditions. The particle size distribution was unaffected by the amount scoured from the bottom or deposited from the flow. Thus, there was no simulation of large particles being deposited in upstream conduits (and thereby unavailable for deposition further downstream). It was not possible to calibrate the routine or even "turn it off" since all constants were incorporated into the program and were not input parameters. Finally, there were situations in which conservation of solids mass was violated. Although the revised routine still represents a gross approximation to the real sediment transport processes at work in sewer systems, it is at least consistent within itself, it conserves mass, and is both calibratable and avoidable.

There have been other recent investigations of solids deposition in sewers, most notably the work of Sonnen (1977) and Pisano et al. (1979). Sonnen's work is highly relevant to the modeling aspect since he developed a deposition-scour routine to accompany the Extran Block of SWMM. This model simulated both bed load and suspended load sediment transport and characterized the sediment by up to ten particle size-specific gravity ranges. Although his routines worked satisfactorily, they are not compatible with the "old" Transport Block, and the "new" Extran Block no longer routes quality parameters. In addition, they are perhaps overly

sophisticated for the present needs. Thus, the current programming utilizes an approximate method that is not as sound as Sonnen's but does have the attributes described earlier.

The best characterization of solids in real sewer systems is given by Pisano et al. (1979) in their description of extensive field and analytical work done in the Boston area. The many problems inherent in dealing with real systems are amply demonstrated.

Methodology and Assumptions

Overview

Since the criterion for deposition and scour depends upon the sediment characteristics (notably size and specific gravity), one option for simulation of the range of characteristics found in real sewer sediment is to carry along a group of different sizes and specific gravities and route each range individually. This is done in the Storage/Treatment Block of SWMM and was done by Sonnen (1977). This has the disadvantage of requiring large array sizes since each range must be simulated for each conduit and preferably for each pollutant.

As an alternative, the present methodology utilizes a fixed particle size distribution and specific gravity (input by the user) for each desired pollutant and maintains a time history for each conduit of the maximum particle diameter (DS) in suspension (really, in motion – via bed or suspended load) and the minimum particle diameter (DB) in the bed. Thus, the particle size distribution of particles in motion is the input distribution truncated on the right at DS, and the particle size distribution of deposited solids is the input distribution truncated on the left at DB. Mass-weighted values of DS are routed downstream for entry to subsequent conduits.

Assumptions

Several assumptions are inherent in the following development, including the following:

1. Solids in sewer systems are assumed to behave like ideal non-cohesive sediment described in various texts (e.g., Graf, 1971; Vanoni, 1975). Unfortunately, the work of Pisano et al. (1979) shows little evidence of this, and, in fact, it may be an impossible task to provide an accurate theoretical description of transport of the highly heterogeneous material constituting "solids" in real sewer systems. The only hope is that the theory will appear to behave in a "reasonable" manner.
2. No distinction is made between particle size distributions resulting from different pollutant sources, e.g., dry-weather flow and storms water. Only one distribution (and one average specific gravity) is used for each pollutant.
3. Shields' criterion is used to determine the dividing particle size between motion and no motion.
4. Once in motion, no distinction is made between bed and suspended load. Particles in motion ("suspension") are routed downstream in each conduit by complete mixing, the same as other quality parameters.
5. When a critical diameter (CRITD) is determined for scour, all particles with diameter less than or equal to CRITD are eroded. There is no effect simulated of armoring or of erosion of layers of the bed.
6. Scour-deposition is considered only in conduits. It is not simulated in non-conduits, including storage elements.

7. The effect of deposited sediment on the bed geometry is not considered. When the hydraulic radius (an important parameter) is calculated to determine the critical diameter for motion, the bed is assumed to have the geometry of the conduit. This leads to some underestimation of deposited material, mainly at low flows.

Shields' Criterion

Shields' diagram for the definition of incipient motion is shown in Figure VI-1. It is widely accepted as a good definition of the beginning of particle motion and describes the balance between the hydrodynamic forces of drag and lift on a particle (tending to induce motion) and the submerged weight of a particle (tending to resist motion). When hydrodynamic forces acting on a sediment particle reach a value such that if increased even slightly will put the particle into motion, critical or threshold conditions are said to have been reached. Dimensional analysis of this condition leads to

$$\frac{\tau_c}{(\gamma_s - \gamma)d} = f\left(\frac{u_* d}{\nu}\right) \qquad \text{(VI-1)}$$

where

τ_c = critical shear stress required to induce particle motion, lb/ft^2
γ_s = specific weight of the sediment, lb/ft^3,
γ = specific weight of water = 62.4 lb/ft^3,
d = sediment diameter, ft (a conversion is made from mm),
u_* = shear or friction velocity, ft/sec, and
ν = kinematic viscosity of water, ft^2/sec.

The equation may be stated in words that the dimensionless critical shear stress is a function of the shear Reynolds number. The critical shear stress and shear velocity are related to each other and to flow properties by

$$u_* = \sqrt{\tau_c / \rho} = \sqrt{g\ R\ S} \qquad \text{(VI-2)}$$

where

ρ = water density = 1.98 slug/ft^3,
g = gravity = 32.2 ft/sec^2,
R = hydraulic radius, ft, and
S = slope of energy grade line (assumed equal to invert slope).

In addition, the specific weight difference may be related to the specific gravity difference between sediment and water,

$$\gamma_s - \gamma = \gamma(SPG - 1) \qquad \text{(VI-3)}$$

where SPG = specific gravity of the sediment, and the specific gravity of water is taken as 1.0.

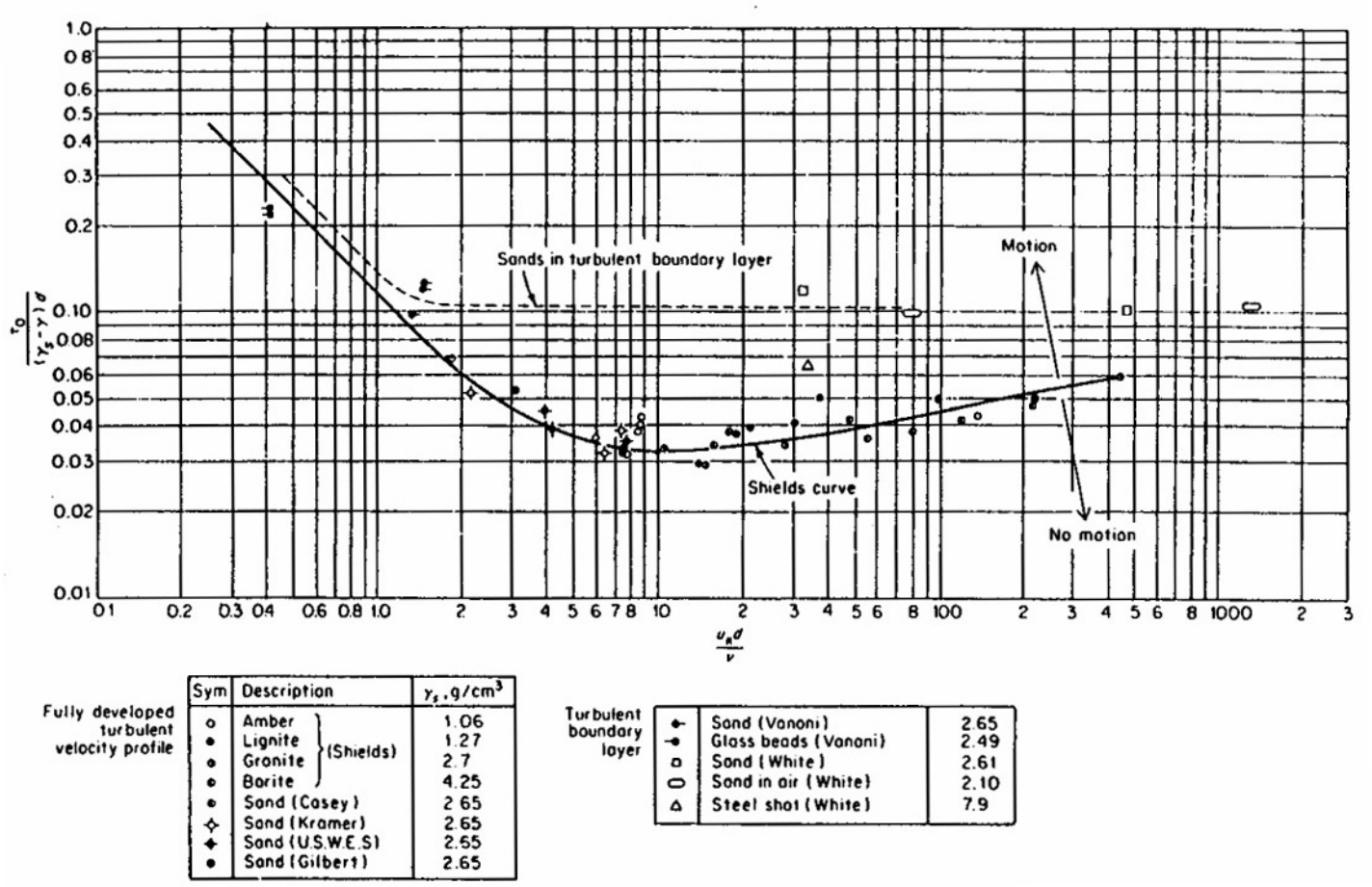

Figure VI-1. Shield's diagram for definition of incipient motion (after Graf, 1971, p. 96).

Experiments on critical shear stress (e.g., see Graf, 1971, and Vanoni, 1975) reveal the motion of sediment grains to be highly unsteady and non-uniformly distributed. Near critical conditions, observations of a large area of the sediment bed will show that the incidence of sediment motion occurs as gusts and is random in both time and space. Shields and others observed the process of initiation of motion to be stochastic in nature, so that there is no true "critical condition" at which motion suddenly begins. In fact, data on critical shear stress are based upon arbitrary definitions of critical conditions by several investigators. Shields himself determined τ_c as the value for zero sediment discharge obtained by extrapolation on a graph of observed sediment discharge versus shear stress.

Although experiments have been performed incorporating various materials (e.g., sand, glass beads, steel shot, minerals), size ranges and specific gravities, the Shields criterion is generally not used for cohesive sediment that may be more characteristic of sewer systems. Nonetheless, it appears to be the only well document criterion for initiation of motion and is utilized in spite of its limitations.

In SWMM, the Shields diagram is used to determine the dividing sediment diameter between motion and no motion. Thus, it is necessary to solve the functional relationship for the critical diameter, d = CRITD. For programming purposes, the diagram is approximated as shown in Figure VI-2, where two straight line segments bound a central polynomial approximation, all on a log-log plot. Letting the dimensionless shear stress ≡ Y, and the shear Reynolds number ≡ R_*, then the functional forms and their best-fit parameters are as follows:

$R_* \leq 1.47$

$$Y = a \cdot R_*^b \qquad \text{(VI-4)}$$

with

a = 0.1166, and
b = $-0.977842 \cong -1$

$1.47 \leq R_* \leq 10$

$$y = a_0 + a_1 \diamond x + a_2 \diamond x^2 + a_3 \diamond x^3 \qquad \text{(VI-5)}$$

where

$$y = \log_{10} \frac{\tau_c}{(\gamma_s - \gamma)d}$$

$$x = \log_{10} R_*$$

and with

a_0 = -0.9078950
a_1 = -1.2326090

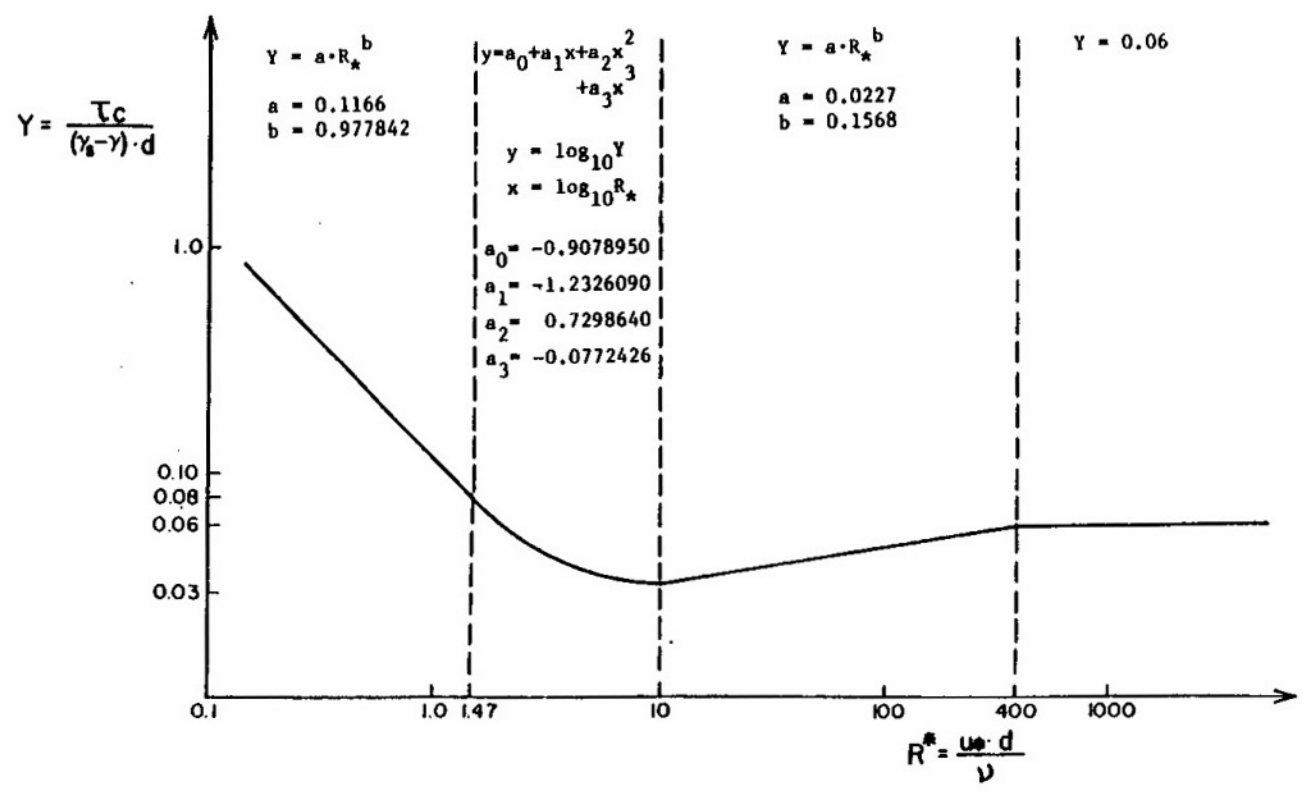

Figure VI-2. Linear and parabolic approximation of Shields' diagram.

a_2 = 0.7298640
a_3 = -0.0772426

$10 \oslash R_* \oslash 400$

$$Y = a \cdot R_*^b \qquad \text{(VI-6)}$$

with

a = 0.0227, and
b = 0.1568

$R_* \leftarrow 400$

$$Y = 0.06 \quad \text{or}$$

$$d = \frac{R \cdot S}{(SPG - 1) \cdot 0.06} \qquad \text{(VI-7)}$$

The straight line segments may be solved directly for the critical diameter from

$$\frac{\tau_c}{(\gamma_s - \gamma)d} = a\left(\frac{u_* d}{\nu}\right)^b \qquad \text{(VI-8)}$$

and using the relationships of equations VI-2 and VI-3, resulting in

$$CRITD = \left[\frac{(R \cdot S)^{1-b/2} \nu^b}{(SPG - 1) \cdot a \cdot g^{b/2}}\right]^{\frac{1}{1+b}} \qquad \text{(VI-9)}$$

Equation VI-9 works well for the coefficients a and b of equation VI-6. But for equation VI-4, $b \cong -1$ and the exponent approaches infinity. For the region $R_* \leq 1.47$, all sediment particles are within the laminar sublayer of the flow, and motion is independent of the diameter (Graf, 1971). For practical purposes, there is no apparent motion, and the critical diameter is assumed to be the value at $R_* = 1.47$ in the model, that is,

$$d = \frac{1.47 \cdot \nu}{\sqrt{RSg}} \ .$$

The polynomial for the transition region, $1.47 \leq R_* \leq 10$, is rapidly solved using a Newton-Raphson iteration. In the program, equation VI-9 is first solved using the a and b values for equation VI-6 ($10 \leq R_* \leq 400$). If the resulting value of R_* is greater than 400, the critical diameter is evaluated from equation VI-7. If R_* is less than 10, the polynomial approximation is then solved. If the resulting value of R_* from polynomial is greater than 10, the critical diameter

is assumed to be the value of $R_* = 10$, and if R_* is less than 1.47, the value at $R_* = 1.47$ is used as a default.

Regarding the parameters of equation VI-9, the slope, S, is taken as the invert slope (SLOPE) for each conduit, used by the Transport Block. The hydraulic radius is calculated at each time step, and the kinematic viscosity (GNU), ν, is input for each run. (It incorporates any temperature effects.) The specific gravity (SPG) of sewer particles ranges from 1.1 for organic material to 2.7 for sand and grit. An average value, based upon the rough composition of the sediment, must be used. When quality parameters are input in card group F1 of the Transport Block, if SPG ≤ 1.0, the deposition-scour routine will not be used. It may be seen that if SPG is greater than 1.0 but very close to it, the value of CRITD in equation VI-9 becomes highly sensitive to it.

Particle Size Distribution

The particle size distribution for each pollutant for which it is desired to simulate deposition and scour is input by up to four straight line segments, as shown in Figure VI-3 (see also Figure 6-6). The distribution may be based upon characteristics of surface sediment for simulation of storm sewers, but should utilize sewer conduit samples for combined sewers.

An example will best illustrate the use of the particle size distribution. Consider first an example of scour. The distribution of Figure VI-3 is sketched again in Figure VI-4a. At the beginning of the time step, all particles in the bed are assumed to have diameters ≥ DB = 0.6 mm in the example. If a new critical diameter, CRITD, is calculated that is greater than DB (CRITD = 1.5 mm in the example), the new bed distribution will become as shown in Figure VI-4b. The percent of the bed mass that is scoured is

$$\frac{72-35}{72}\times 100 = 51\%$$

(Under the original methodology in the Transport Block, it would have been assumed that 100-35 or 65 percent of the mass of the bed would be scoured.)

A similar calculation applies to deposition. If the suspended material (particles in motion) have the distribution shown in Figure VI-4c, it becomes that of Figure VI-4d. The percent of the suspended load that is deposited is

$$\frac{56-34}{100-34}\times 100 = 33\%$$

(Under the original methodology in the Transport Block, it would have been assumed that 56 percent of the suspended load would be deposited.) When scoured material is added to suspended material, a new value of DS is computed by mass-weighting:

$$DS_2 = \frac{DS_1 \cdot M_s + CRITD \cdot M_e}{M_s + M_e} \qquad \text{(VI-10)}$$

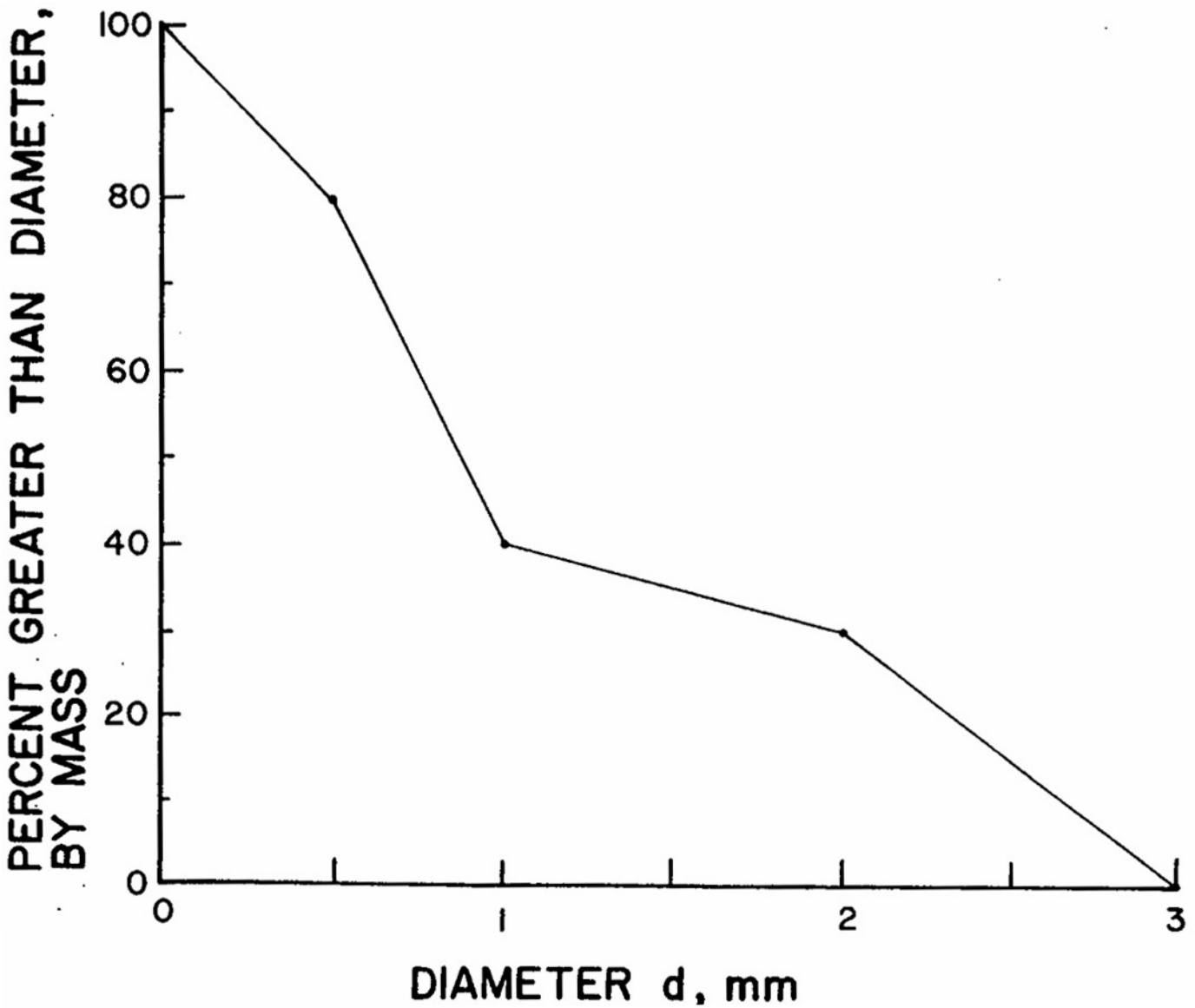

Figure VI-3. Particle size distribution for a pollutant.

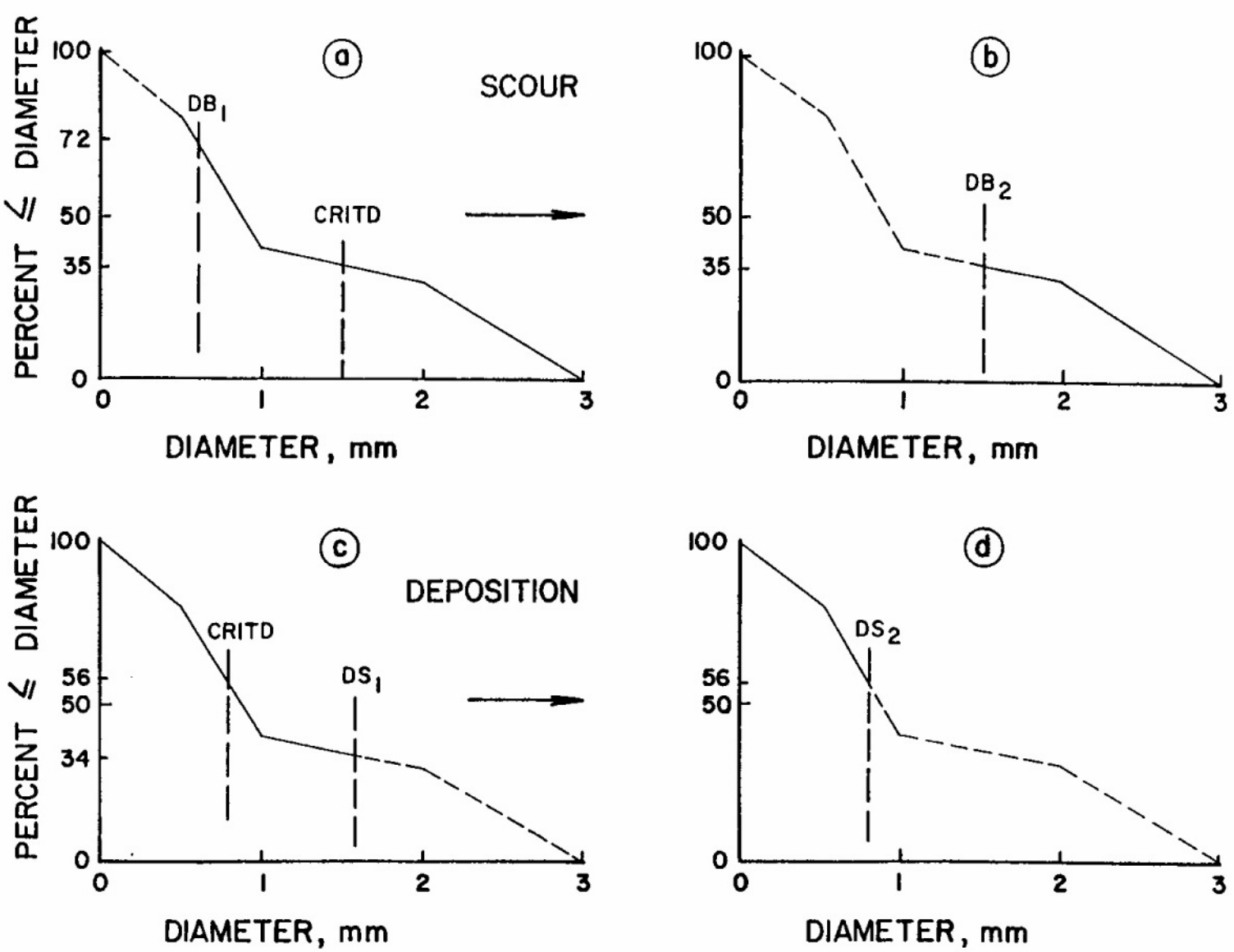

Figure VI-4. Truncation of particle size distribution during scour and deposition.

where

DS_2 = new value of DS, mm
DS_1 = old value of DS, mm
M_s = original mass in suspension, mg, and
M_e = mass eroded from bed, mg.

Similarly, if suspended material is deposited,

$$DB_2 = \frac{DB_1 \cdot M_b + CRITD \cdot M_d}{M_b + M_d} \qquad \text{(VI-11)}$$

where

DB_2 = new value of DB, mm,
DB_1 = old value of DB, mm,
M_b = original mass of bed material, mg, and
M_d = mass deposited from flow, mg.

Due to this weighting, ordinarily it will not be true that DB = DS even though the same critical diameter, CRITD, applies to both.

Another reason why DB will not necessarily equal DS results from the condition in which CRITD < DB_1 for scour (or CRITD > DS_1 for deposition). In these cases $DB_2 = DB_1$ (or $DS_2 = DS_1$), prior to addition of mass from the flow (or bed), since no mass would be lost from the bed (or from the suspended material).

Inflows and Junctions

To allow some difference between surface inflows to the sewer system and dry-weather flow inflows (e.g., domestic sewage) a maximum particle size, PSDWF, may be specified (in card group F1) for the pollutant found in DWF. This also applies to pollutants entering as a base flow in manholes. Pollutants entering via infiltration are assumed to be completely dissolved and have "zero particle sizes."

At junctions (manholes or other non-conduits), a new value of DS is computed by mass weighting the merging values. For instance,

$$DS_m = \frac{\sum_{i=1}^{3} DS_{u_i} \cdot Q_{u_i} \cdot C_{u_i} + PSDWF \cdot Q_{DWF} \cdot C_{DWF}}{\sum_{i=1}^{3} Q_{u_i} \cdot C_{u_i} + Q_{DWF} \cdot C_{DWF} + Q_{inf}} \qquad \text{(VI-12)}$$

where

DS_m = value of DS of mixture, mm
DS_{u_i} = DS value in upstream conduit i, mm,

Q_{u_i} = outflow from upstream conduit i, cfs,

C_{u_i} = concentration in upstream conduit i, mg/l, and

subscripts DWF and inf refer to dry-weather flow and infiltration, respectively.

Appendix IX

Integrated Form of Complete Mixing Quality Routing

Quality routing in the Transport and Runoff Blocks through conduit segments has long been accomplished by assuming complete mixing within the conduit in the manner of a continuously stirred tank reactor or "CSTR". The procedure is described in the original SWMM documentation (Metcalf and Eddy et al., 1971a, Appendix B) and is very similar to the complete mixing formulation of the Storage/Treatment Block. See, for example, the discussion of equations IV-9, IV-10 and IV-11 in Appendix IV. For the finite difference scheme of equation IV-11, however, it may easily be shown that negative concentrations may be predicted if:

$$\Delta t > \frac{2V}{Q} \tag{IX-1}$$

where

Δt	=	time step, sec,
V	=	average volume in the conduit or storage unit, ft^3, and
Q	=	average flow through the conduit or storage unit, cfs.

This rarely causes a problem for storage unit simulation due to their large volumes. But when long time steps (e.g., 1 hr) are used in Runoff or Transport, instabilities in the predicted concentrations may arise.

These may readily be avoided with minimal loss of accuracy by using the integrated form of the solution to the differential equation. The procedure is described by Medina et al. (1981) and is outlined below as applied to the Runoff and Transport Blocks.

The governing differential equation for a completely mixed volume is

$$\frac{dVC}{dt} = V\frac{dc}{dt} + C\frac{dV}{dt} = Q_i C_i - QC - KCV + L \tag{IX-2}$$

where

C	=	concentration in effluent and in the mixed volume, e.g., mg/l,
V	=	volume, ft^3,
Q_i	=	inflow rate, cfs,

C_i = concentration of influent, e.g. mg/l,
Q = outflow rate, cfs,
K = first order decay coefficient, 1/sec, and
L = source (or sink) of pollutant to the mixed volume, mass/time, e.g. cfs⟐mg/l

An analysis solution of this equation is seldom possible when Q, Q_i, C_i, V and L vary arbitrarily with time, as in the usual routing through conduits. However, a simple solution is available to the ordinary, first order differential equation with constant coefficients if parameters Q, Q_i, C_i, V, L and dV/dt are assumed to be constant over the solution time interval, t to t + Δt. In practice, average values over the time interval are used at each time step. Equation IX-2 is then readily integrated over the time interval t to t + Δt with

$$C(0) = C(t) \tag{IX-3}$$

to yield

$$C(t+\Delta dt) = \left(\frac{\frac{Q_i C_i + L}{V}}{DNOM} \right) \left(1 - e^{-DENOM \cdot \Delta t}\right) + C(t)\ e^{-DENOM \cdot \Delta t} \tag{IX-4}$$

where

$$DENOM = Q/V + K + \frac{1}{V} dV/dt \tag{IX-5}$$

Thus, the concentration at the end of the time step is predicted as the sum of a weighted inflow concentration and a decaying concentration from the previous time step.

Equation IX-4 is used in both the Runoff and Transport Block and is completely stable with respect to changes in Δt. It does not reflect rapid changes in volume and flow as well as the finite difference solution (e.g., equation IV-11) but it is updated at each time step. Given the many other uncertainties of quality routing within the sewer system, it should be adequate.

Appendix X

Subsurface Flow Routing in Runoff Block

Introduction

Because SWMM was originally developed to simulate combined sewer overflows in urban catchments, the fate of infiltrated water was considered insignificant. Since its development, however, SWMM has been used on areas ranging from highly urban to relatively undeveloped. Many of the undeveloped and even some of the developed areas, especially in areas like south Florida, are very flat with high water tables, and their primary drainage pathway is through the surficial groundwater aquifer and the unsaturated zone above it, rather than by overland flow. In these areas a storm will cause a rise in the water table and subsequent slow release of groundwater back to the receiving water (Capece et al., 1984). For this case, the fate of the infiltrated water is highly significant. By assuming that the infiltration is lost from the system, an important part of the high-water-table system is not being properly described (Gagliardo, 1986).

It is known that groundwater discharge accounts for the time-delayed recession curve that is prevalent in certain watersheds (Fetter, 1980). This process has not, however, been satisfactorily modeled by surface runoff methods alone. By modifying infiltration parameters to account for subsurface storage, attempts have been made to overcome the fact that SWMM assumes infiltration is lost from the system (Downs et al., 1986). Although the modeled and measured peak flows matched well, the volumes did not match well, and the values of the infiltration parameters were unrealistic. Some research on the nature of the soil storage capacity has been done in south Florida (SFWMD, 1984). However, it was directed towards determining an initial storage capacity for the start of a storm. There remains no standard, widely-used method for combining the groundwater discharge hydrograph with the surface runoff hydrograph and determining when the water table will rise to the surface. For instance, HSPF (Johansen et al., 1980) performs extensive subsurface moisture accounting and works well during average conditions. However, the model never permits the soil to become saturated so that no more infiltration is permitted, limiting its usefulness during times of surface saturation and flooding. Another difficulty with HSPF occurs during drought conditions, since there is no threshold saturated zone water storage (corresponding to the bottom of a stream channel) below which no saturated zone outflow will occur. These difficulties have limited HSPF usefulness for application to extreme hydrologic conditions in Florida (Heaney et al., 1986).

In order to incorporate subsurface processes into the simulation of a watershed and overcome previously mentioned shortcomings, SWMM has been equipped with a simple

groundwater subroutine. The remainder of this appendix will describe the theory, use, and some limitations of the subroutine.

Theory

Introduction

An effort was made to utilize existing theoretical formulations for as many processes as possible. The purpose was to maintain semblance to the real world while enabling the user to determine parameter values that have meaning to the soil scientist. Also, in the following discussion the term "flow" will refer to water that is passed on to another part of the system, and the term "loss" will refer to water that is passed out of the system. In addition, in the groundwater subroutines, flows and losses have internal units of velocity (flow per unit area).

The groundwater subroutine, GROUND, simulates two zones – an upper (unsaturated) zone and a lower (saturated) zone. This configuration is similar to the work done by Dawdy and O'Donnell (1965) for the USGS. The flow from the unsaturated to the saturated zone is controlled by a percolation equation for which parameters may either be estimated or calibrated, depending on the availability of the necessary soil data. Upper zone evapotranspiration is the only loss from the unsaturated zone. The only inflow to subroutine GROUND is the calculated infiltration from subroutine WSHED. Losses and outflow from the lower zone can be via deep percolation, saturated zone evapotranspiration, and groundwater flow. Groundwater flow is a user-defined power function of water table stage and, if chosen, depth of water in the discharge channel.

Continuity

The physical processes occurring within each zone are accounted for by individual mass balances in order to determine end-of-time-step stage, groundwater flow, deep percolation, and upper zone moisture. Parameters are shown in Figure X-1 and defined below. Mass balance in the upper (unsaturated) zone is given by,

$$TH2 = \left\{ \begin{matrix} \left[(ENFIL - ETU) \cdot PAREA - PERC \right] \\ \cdot DELT + (D1 - D2) \cdot TH2 + TH \cdot DWT1 \end{matrix} \right\} \Big/ (DTOT - D2) \qquad \text{(X-1)}$$

In the lower (saturated) zone, for rising water tables,

$$D2 = \left\{ \begin{matrix} \left[\begin{matrix} PERC - ETD \cdot PAREA - .5 \\ \cdot \left(\begin{matrix} GWFKW + A1 \cdot (D2 - BC)^{B1} + A3 \\ \cdot D2 \cdot TW + DEPRC + DP \cdot D2/DTOT \end{matrix} \right) - TWFFLW \end{matrix} \right] \\ DELT + (D2 - D1) \cdot (TH - TH2) \end{matrix} \right\} \Big/ (PR - TH2) + D1 \qquad \text{(X-2)}$$

and for falling water tables,

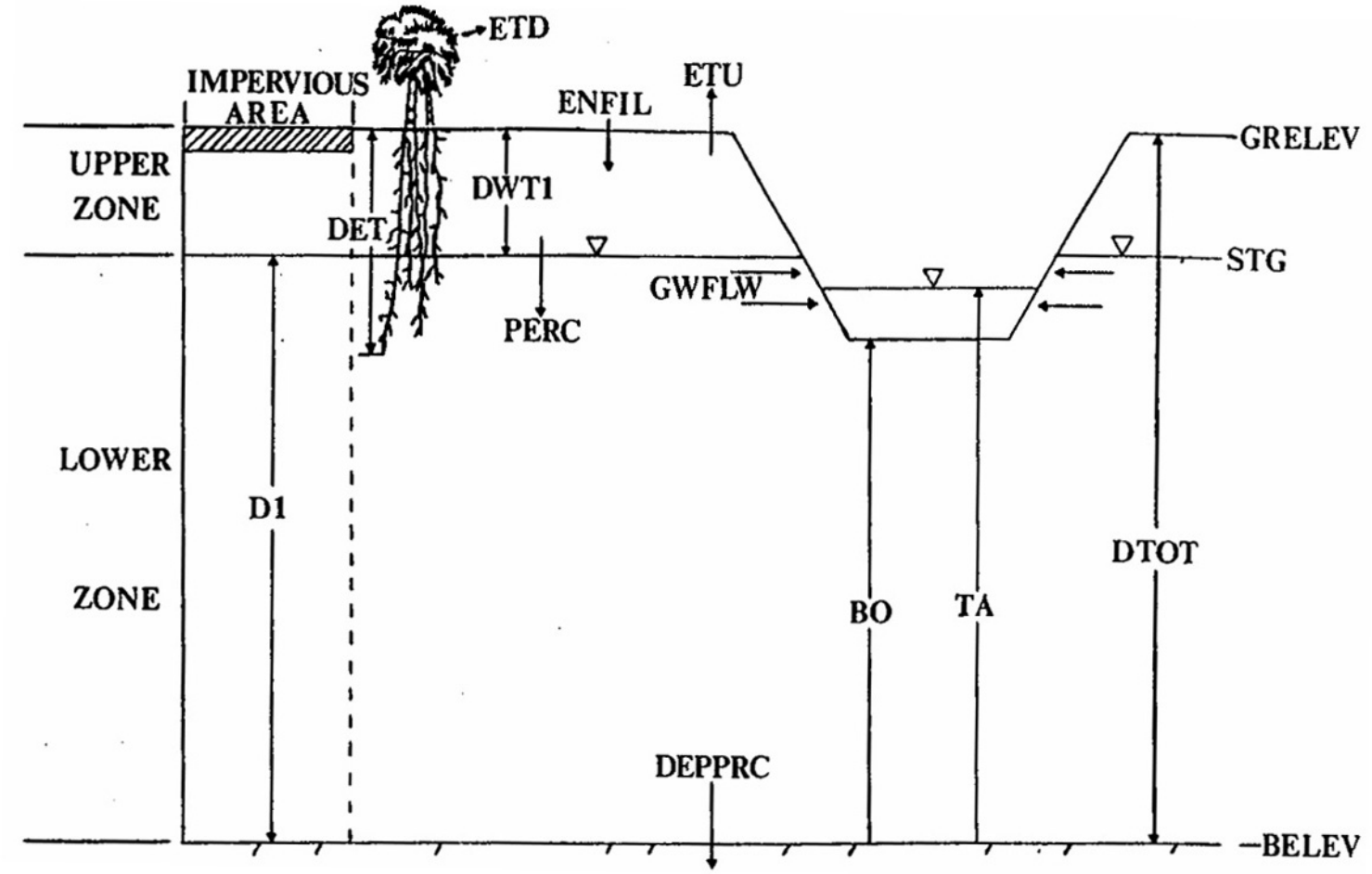

Figure X-1. GROUND parameters and conceptualization.

$$\left\{\left[\begin{array}{l}\text{PERC}-\text{ETD}\cdot\text{PAREA}-.5\\ \left(\begin{array}{l}\text{GWFLW}+\text{A1}\cdot(\text{D2}-\text{BC})^{\text{B1}}+\text{A3}\\ \cdot\,\text{D2}\cdot\text{TW}+\text{DEPPRC}+\text{DP}\cdot\text{D2}/\text{DTOT}\end{array}\right)-\text{TWFLW}\end{array}\right]\cdot\text{DELT}\right\}\Big/(\text{PR}-\text{TH2})+\text{D1} \qquad \text{(X-3)}$$

where

TH2	=	end-of-time-step upper zone moisture content (fraction),
ENFIL	=	infiltration rate calculated in subroutine WSHED,
ETU	=	upper zone evapotranspiration rate,
PERC	=	percolation rate,
PAREA	=	pervious area divided by total area,
DELT	=	time step value,
D	=	beginning-of-time-step lower zone depth (elevation above a datum),
D2	=	end-of-time-step lower zone depth,
TH	=	beginning-of-time-step upper zone moisture content,
DWT1	=	beginning-of-time-step upper zone depth,
DTOT	=	total depth of upper and lower zone = D1+DWT1,
ETD	=	lower zone evapotranspiration rate,
GWFLW	=	beginning-of-time-step groundwater flow rate,
A1	=	groundwater flow coefficient,
BC	=	bottom of channel depth (elevation above datum),
B1	=	groundwater flow exponent,
DEPPRC	=	beginning-of-time-step deep percolation rate,
DP	=	a recession coefficient derived from interevent declines in the water table,
PR	=	porosity, and
TWFLW	=	channel water influence rate,
A3	=	groundwater flow coefficient, and
TW	=	depth of water in channel (elevation above datum).

Moisture content (a fraction) is defined as the volume of moisture divided by the volume of solids plus voids. The maximum possible moisture content is the porosity; the minimum is the wilting point (discussed below). Solving equation X-1 for TH2 and using DWT1 = DTOT-D1, yields a much simpler form which is not a function of the unknown D2,

$$\text{TH2}=[(\text{ENFIL}-\text{ETU})\cdot\text{PAREA}-\text{PERC}]\cdot\text{DELT}/\text{DWT1}+\text{TH} \qquad \text{(X-4)}$$

Equation X-4 is solved first, followed by a Newton-Raphson solution of equation X-2 or X-3. The sequencing will be described in more detail in a subsequent section, following a description of the various simulated processes.

Infiltration

Infiltration enters subroutine GROUND as the calculated infiltration from subroutine WSHED. As before in SWMM, either the Horton or Green-Ampt equation can be used to describe infiltration. For time steps where the water table has risen to the surface, the amount of infiltration that cannot be accepted is subtracted from RLOSS (infiltration plus surface evaporation) in subroutine WSHED. In the event that the infiltrated water is greater than the amount of storage available for that time step, the following equation is used to calculate the amount of infiltration that is not able to be accepted by the soil.

$$XSINFL = ENVIL \cdot DELT - AVLVOL/PAREA \qquad (X\text{-}5)$$

where

XSINFL = excess infiltration over pervious area, and
AVLVOL = initial void volume in the upper zone plus total losses and outflows from the system for the time step.

The second condition exists because of the algebra in equations X-2, X-3 and X-4. As the water table approaches the surface, the end-of-time-step moisture value, TH2, approaches the value of porosity, which makes the denominator in equations X-2 and X-3 go towards zero. Since a denominator close to zero could result in an unrealistic value of D2, a different way of handling the calculations had to be implemented. When the initial available volume in the upper zone plus the volume of total outflows and losses from the system minus the infiltration volume is between zero and an arbitrary value of 0.0001 ft, several assumptions are made. First, end-of-time-step groundwater flow and deep percolation, which are normally found by iteration, are assumed to be equal to their respective beginning-of-time-step values. This step is taken to ensure that the final available volume remains in the previously mentioned range. Second, TH2 is set equal to an arbitrary value of 90% of porosity. It is believed that this will allow the TH2 value in this special case to be reasonably consistent with the TH^2 values juxtaposed to it in the time series. Third, D2 is set close to the total depth – the actual value of D2 depends on the value of porosity. Fourth, the amount of infiltration that causes the final available volume to exceed 0.0001 ft is calculated in the following equation and sent back to the surface in the form of a reduction in the term RLOSS in subroutine WSHED.

$$XSINFL = ENFIL \cdot DELT + (.0001 - AVLVOL)/PAREA \qquad (X\text{-}6)$$

Because of the way this special case is handled, it is possible for a falling water table to have the calculated excess infiltration be greater than the actual amount of infiltration. It is not desirable for the ground to pump water back onto the surface! Hence, the difference between the calculated excess infiltration and the actual infiltration is added to the infiltration value of the next time step. The number of occurrences of this situation in a typical run is very small, as is the computed difference that is passed to the next time step, so no problems should occur because of this solution.

Upper Zone Evapotranspiration

Evapotranspiration from the upper zone (ETU) represents soil moisture lost via cover vegetation and by direct evaporation from the pervious area of the subcatchment. No effort was made to derive a complex formulation of this process. The hierarchy of losses by evapotranspiration is as follows: 1) surface evaporation, 2) upper zone evapotranspiration, and 3) lower zone transpiration. Upper zone evapotranspiration is represented by the following equations,

ETMAX = VAP(MONTH) (X-7)

ETAVLB = ETMAX-EVAPO (X-8)

ETU = CET*ETMAX (X-9)

IF(TH.LT.WP.OR.ENFIL.GT.O.) ETU = 0. (X-10)

IF(ETU.GT.ETAVLB) ETU = ETAVLB (X-11)

where

ETMAX	=	maximum total evapotranspiration rate (input on card F1),
VAP(MONTH)	=	input maximum evapotranspiration rate for month MONTH,
ETAVLB	=	maximum upper zone evapotranspiration rate,
EVAPO	=	portion of ETMAX used by surface water evaporation,
CET	=	fraction of evapotranspiration apportioned to upper zone, and
WP	=	wilting point of soil.

The two conditions that make ETU equal to zero in equation X-10 are believed to simulate the processes actually occurring in the natural system. The first condition (moisture content less than wilting point) relates to the soil science interpretation of wilting point – the point at which plants can no longer extract moisture from the soil. The second condition (infiltration greater than zero) assumes that vapor pressure will be high enough to prevent additional evapotranspiration from the unsaturated zone.

Lower Zone Evapotranspiration

Lower zone evapotranspiration, ETD, represents evapotranspiration from the saturated zone over the pervious area. ETD is the last evapotranspiration removed, and is determined by the following depth-dependent equation and conditions.

ETD = (DET-DWT1)*ETMAX*(1-CET)/DET (X-12)

IF(ETD.GT.(ETAVLB-ETU)) ETD = ETAVLB-ETU (X-13)

IF(ETD.LT.0.) ETD = 0. (X-14)

where

ETD = lower zone evapotranspiration rate, and
DET = depth over which evapotranspiration can occur.

Since ETD is typically very small compared to other terms and has to be checked for certain conditions, it is assumed constant over the time step and not solved for in the iterative process.

Percolation

Percolation (PERC) represents the flow of water from the unsaturated zone to the saturated zone, and is the only inflow for the saturated zone. The percolation equation in the subroutine was formulated from Darcy's Law for unsaturated flow, in which the hydraulic conductivity, K, is a function of the moisture content, TH. For one-dimensional, vertical flow, Darcy's Law may be written

$$v = -K(TH) \diamond dh/dz \qquad \text{(X-15)}$$

where

v = velocity (specific discharge) in the direction of z,
z = vertical coordinate, positive upward,
K(TH) = hydraulic conductivity,
TH = moisture content, and
h = hydraulic potential.

The hydraulic potential is the sum of the elevation (gravity) and pressure heads,

$$h = z + PSI \qquad \text{(X-16)}$$

where PSI = soil water tension (negative pressure head) in the unsaturated zone.

Equating vertical velocity to percolation, and differentiating the hydraulic potential, h, yields

$$\text{Percolation} = -K(TH) \diamond (1 + dPSI/dz) \qquad \text{(X-17)}$$

A choice is customarily made between using the tension, PSI, or the moisture content, TH, as parameters in equations for unsaturated zone water flow. Since the quantity of water in the unsaturated zone is identified by TH in previous equations, it is the choice here. PSI can be related to TH if the characteristics of the unsaturated soil are known. Thus, for use in equation X-17, the derivative is

$$dPSI/dz = dPSI/dTH \diamond dTH/dz \qquad \text{(X-18)}$$

The slope of the PSI versus TH curve should be obtained from data for the particular soil under consideration. Relationships for a sand, sandy loam and silty loam are shown in Figures X-2, X-3 and X-4 (Laliberte et al., 1966). The data are based on laboratory tests of disturbed soil samples and illustrate only the desaturation (draining) characteristics of the soil. The relationship during the saturation (wetting) phase will ordinarily be different; when both the wetting and draining relationships are shown the curves usually illustrate a hysteresis effect. The figures also show the relationship between the hydraulic conductivity of the unsaturated soils and the moisture content. In some cases (e.g., sand), K(TH) may range through several orders of magnitude. Soils data of this type are becoming more readily available; for example, soil science departments at universities often publish such information (e.g., Carlisle et al., 1981). The data illustrated in Figures X-2, X-3 and X-4 are also useful for extraction of parameters for the Green-Ampt infiltration equations.

Equation X-17 may be approximated by finite differences as

$$\text{Percolation} = -K(TH) \diamond [1+(\Delta TH/\Delta z)\diamond(\Delta PSI/\Delta TH)] \quad \text{(X-19)}$$

For calculation of percolation, it is assumed that the gradient, $\Delta TH/\Delta z$, is the difference between moisture content TH in the upper zone and field capacity at the boundary with the lower zone, divided by the average depth of the upper zone, DWT1/2. Thus,

$$\text{Percolation} = -K(TH) \diamond \{1+[(TH-FD)\diamond 2/DWT1] \diamond PCO\} \quad \text{(X-20)}$$

where

FD = field capacity, and
PCO = $\Delta PSI/\Delta TH$ in the region between TH and FD.

PCO is obtained from data of the type of Figures X-2, X-3 and X-4.

Finally, the hydraulic conductivity as a function of moisture content is approximated functionally in the moisture zone of interest as

$$K(TH) = HKTH = HKSAT \diamond EXP[(TH-PR)\diamond HCO] \quad \text{(X-21)}$$

where

HKTH = hydraulic conductivity as a function of moisture content,
HKSAT = saturated hydraulic conductivity, and
HCO = calibration parameter.

HCO can be estimated by fitting the HKTH versus TH curve to the hydraulic conductivity versus moisture content curve, if such data are available (e.g., Figures X-2, X-3, X-4); three fits are shown in Figure X-5. The fits are not optimal over the entire data range because the fit is only

performed for the high moisture content region between field capacity and porosity. If soils data are not available, HCÏ can be estimated by model calibration.

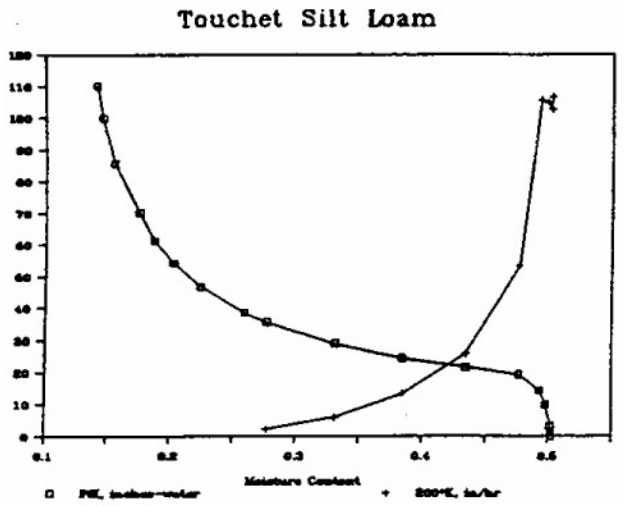

Figure X-2. Tension, PSI (squares, in. of water) and hydraulic conductivity, K (crosses, in./hr, K multiplied by 200) versus moisture content. Derived from data of Laliberte et al. (1966), Tables B-5 and C-3. Porosity = 0.503, temp. = 26.5° C, saturated hyd. conductivity = 0.53 in./hr.

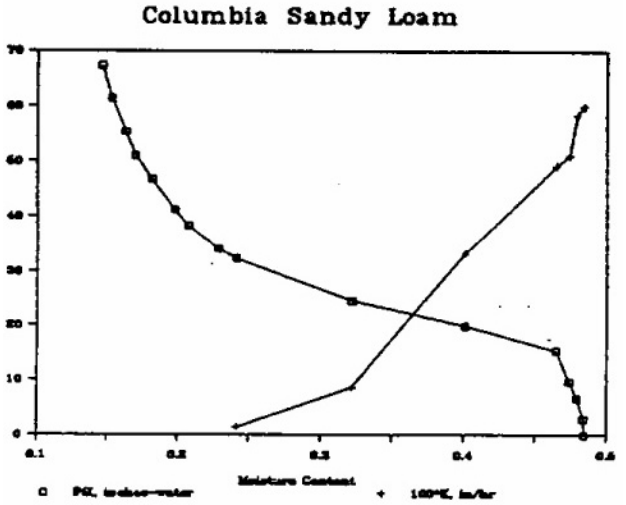

Figure X-3. Tension, PSI (squares, in. of water) and hydraulic conductivity, K (crosses, in./hr, K multiplied by 100) versus moisture content. Derived from data of Laliberte et al. (1966), Tables B-8 and C-5. Porosity = 0.485, temp. = 25.1 °C, saturated hyd. conductivity = 0.60 in./hr.

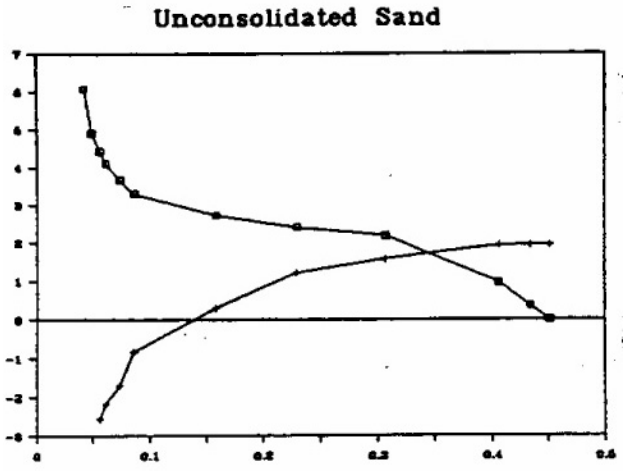

Figure X-4. Tension, PSI (squares, in. of water) and log-10 of hydraulic conductivity, K (crosses, K in in./hr) versus moisture content. Derived from data of Laliberte et al. (1966), Tables B-14 and C-11. Porosity = 0.452, temp. = 25.1°C, saturated hyd. conductivity = 91.5 in./hr.

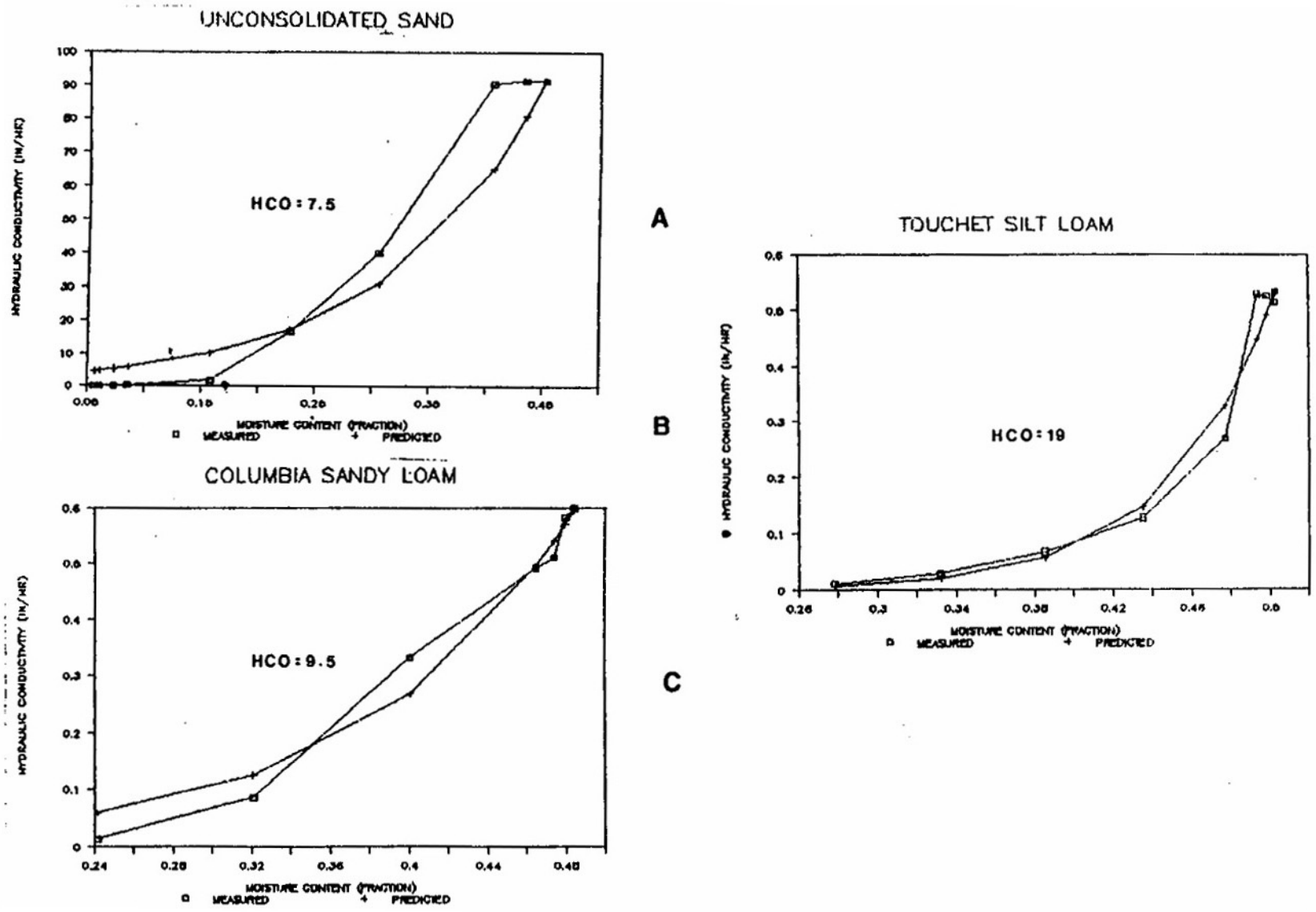

Figure X-5. Model representation and measured hydraulic conductivity curves for three types of soil.

Combining equations X-20 and X-21 gives the resulting percolation equation for the model,

$$PERC = HKTH \diamond [1+PCO \diamond (TH-FD)/(DWT1/2)] \quad (X\text{-}22)$$

where PERC = percolation rate (positive downward) and is only nonzero when TH is greater than FD.

If data sources for parameters PCO and HCO are lacking, they may be estimated through the calibration process. On the basis of preliminary runs, the groundwater subroutine is relatively insensitive to changes in PCO and HCO, so a lack of extensive soils data should not discourage one from using the model.

If moisture content is less than or equal to field capacity, percolation becomes zero. This limit is in accordance with the concept of field capacity as the drainable soil water that cannot be removed by gravity alone (Hillel, 1982, p. 243). Once TH drops below field capacity, it can only be further reduced by upper zone evapotranspiration (to a lower bound of the wilting point).

The percolation rate calculated by equation X-22 will be reduced by the program if it is high enough to drain the upper zone below field capacity or make the iterations for D2 converge to an unallowable value. Also, since checks must be made on PERC, it is assumed to be constant over the time step and therefore not determined through an iterative process.

Field Capacity and Wilting Point

These parameters are used for demarcations for percolation and ET. Field capacity, FC, is usually considered to be the amount of water a well-drained soil holds after free water has drained off, or the maximum amount it can hold against gravity (SCS, 1964; Linsley et al., 1982). This occurs at soil moisture tensions (see further discussion below) of from 0.1 to 0.7 atmospheres, depending on soil texture. Moisture content at a tension of 1/3 atmosphere is often used. The wilting point (or permanent wilting point), WP, is the soil moisture content at which plants can no longer obtain enough moisture to meet transpiration requirements; they wilt and die unless water is added to the soil. The moisture content at a tension of 15 atmospheres is accepted as a good estimate of the wilting point (SCS, 1964; Linsley et al., 1982). The general relationship among soil moisture parameters is shown in Figure X-6 (SCS, 1964).

Data for FC and WP are available from the SCS, agricultural extension offices and university soil science departments. Generalized data are shown in Table X-1, as derived from Linsley et al. (1982, p. 179).

Deep Percolation

Deep percolation represents a lumped sink term for unquantified losses from the saturated zone. The two primary losses are assumed to be percolation through the confining layer and lateral outflow to somewhere other than the receiving water. The arbitrarily chosen equation for deep percolation is

$$DEPPRC = DP \diamond D1/DTOT \quad (X\text{-}23)$$

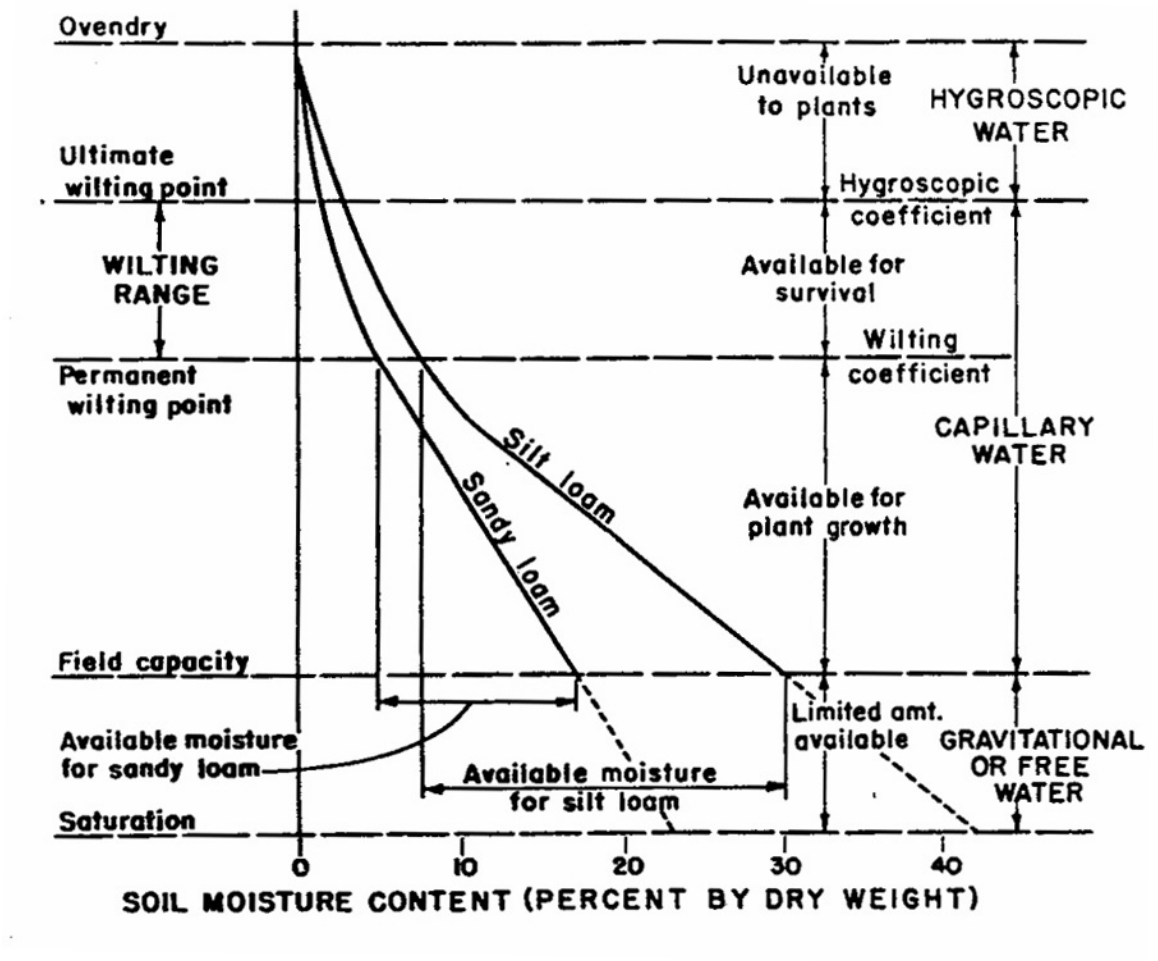

Figure X-6. Kinds of water in soil (SCS, 1964). Note that silt loam contains more than twice as much readily available water than sandy loam.

Table X-1. Volumetric Moisture Content at Field Capacity and Wilting Point (derived* from Linsley et al., 1982, Table 6-1.)

Soil Type	Field Capacity	Wilting Point
Sand	0.08	0.03
Sandy loam	0.17	0.07
Loam	0.26	0.14
Silt Loam	0.28	0.17
Clay loam	0.31	0.19
Clay	0.36	0.26
Peat	0.56	0.30

*Fraction moisture content = fraction dry weight × dry density / density of water.

where

DEPPRC = beginning-of-time-step deep percolation rate, and
DP = a recession coefficient derived from interevent water table recession curves.

The ratio of D1 to DTOT allows DEPPRC to be a function of the static pressure head above the confining layer. Although DEPPRC will be very small in most cases, it is included in the iterative process so that an average over the time step can be used. By doing this, large continuity errors will be avoided should DEPPRC be set at a larger value.

Groundwater Discharge

Functional Form

Groundwater discharge represents lateral flow from the saturated zone to the receiving water. The flow equation takes on the following general form:

$$GWFLW = A1 \diamond (D1-BC)^{B1} - TWFLW + A3 \diamond D1 \diamond TW \quad \text{(X-24)}$$

and

$$TWFLW = A2 \diamond (TW-BC)^{B2} \quad \text{(X-25)}$$

where

GWFLW = beginning-of-time-step groundwater flow rate (per subcatchment area,
TWFLW = channel water influence flow rate (per subcatchment area),
A1,A2 = groundwater and channel water influence flow coefficients,

A3	=	coefficient for cross-product,
B1,B2	=	groundwater and tailwater influence flow exponents,
BC	=	elevation of bottom of channel, and
TW	=	elevation of water in channel.

If D1 is less than BC or TW, GWFLW is set equal to zero. In addition, if TW = BC and B2 = 0, then the indeterminant form of zero raised to the zero power in equation X-25 is set equal to 1.0 by the program. The functional form of equations X-24 and X-25 was selected in order to be able to approximate various horizontal flow conditions, as will be illustrated below.

Since groundwater flow can be a significant volume, an average flow each time step is found by iteration using equation X-2 or X-3. Groundwater flows can be routed to any previously defined inlet, trapezoidal channel, or pipe, al-lowing the user to isolate the various components of the total hydrograph, as shown in Figure X-7. That is, the groundwater flow does not have to be routed to the same destination as the overland flow from the subcatchment.

The effects of channel water on groundwater flow can be dealt with in two different manners. The first option entails setting TW (elevation of water surface in the channel) to a constant value greater than or equal to BC (bottom-of-channel elevation) and A2, B2 and/or A3 to values greater than zero. If this method is chosen, then the user is specifying an average tailwater influence over the entire run to be used at each time step.

The second option makes the channel water elevation, TW, equal to the elevation of water in an actual channel (trapezoidal channel or circular pipe). For this option, the groundwater must be routed to a trapezoidal channel or pipe – not an inlet. The depth of water in the channel (TW - BC) at each time step is then determined as the depth in the channel or pipe from the previous time step. (It is assumed that the bottom of the channel is at the elevation BC.) The beginning-of-time-step depth must be used to avoid complex and time-consuming iterations with the coupled channel discharge equations in subroutine GUTTER. Unfortunately, because of this compromise the groundwater flow may pulsate as D1 oscillates between just above and just below elevation TW. This pulsing may introduce errors in continuity and is, of course,

Figure X-7. Hydrograph of total flow and its two major components.

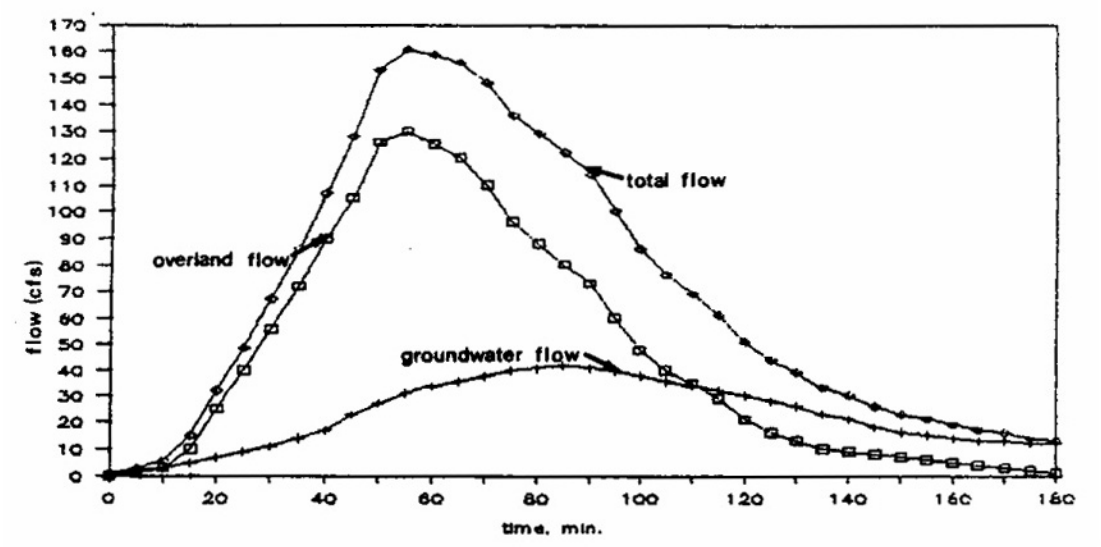

unrepresentative of the actual system. Shorter time steps and larger or less steep channels (reducing the response of the channel) can be used to reduce the pulses. Also, caution must be taken when selecting A1, B1, A2, B2 and A3 so that GWFLW cannot be negative. Although this may occur in the actual system and represent recharge from the channel, there is currently no means of representing this reverse flow and subtracting it from the channel. One way of assuring that this cannot happen is to make A1 greater than or equal to A2 and B1 greater than or equal to B2, and A3 equal to zero.

Because of the general nature of the equation, it can take on a variety of functional forms. For example, a linear reservoir can be selected by setting B1 equal to one and A2 and A3 equal to zero. Two drainage examples are illustrated below.

Example: Infiltration and Drainage to Adjacent Channel

Under the assumption of uniform infiltration and horizontal flow by the Dupuit-Forcheimer approximation, the relationship between water table elevation and infiltration for the configuration shown in Figure X-8 is (Bouwer, 1978, p. 51)

$$K\left(h_1^2 - h_2^2\right) = L^2 f \qquad \text{(X-26)}$$

where

f = infiltration rate,
K = hydraulic conductivity, and other parameters are as shown on Figure X-8.

Before matching coefficients of equations X-24 and X-25 to equation X-26, it should be recognized that the water table elevation in SWMM, D1, represents an <u>average</u> over the catchment, not the maximum at the "upstream" end that is needed for h_1 in equation X-26. Let D1 be the average head,

$$D1 = \left(h_1 + h_2\right)/2 \qquad \text{(X-27)}$$

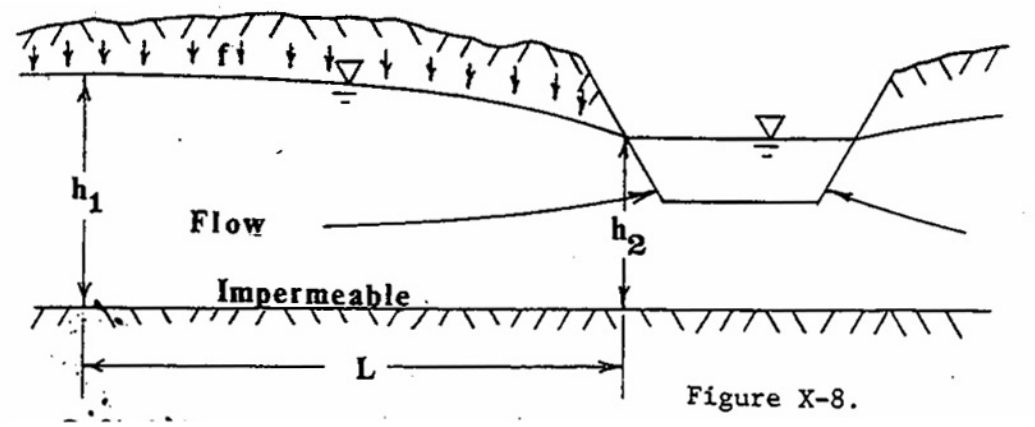

Figure X-8. Definition sketch for Dupuit-Forcheimer approximation for drainage to adjacent channel.

Substituting $h_1 = 2\,D1 - h_2$ into equation X-26 gives, after algebra

$$\left(D1^2 - D1\,h_2\right) 4K/L^2 = f \tag{X-28}$$

from which a comparison with equations X-24 and X-25 yields $A1 = A3 = 4K/L^2$, $A2 = 0$, and $B1 = 2$. Note that GWFLW has units of flow per unit area, or length per time, which are the units of infiltration, f, in equation X-28.

Example: Hooghoudt's Equation for Tile Drainage

The geometry of a tile drainage installation is illustrated in Figure X-9. Hooghoudt's relationship (Bouwer, 1978, p. 295) among the indicated parameters is

$$f = \left(2D_e + m\right) 4Km/L^2 \tag{X-29}$$

where D_e = effective depth of impermeable layer below drain center, and other parameters are defined in Figure X-9. D_e is less than or equal to b_o in Figure X-9 and is a function of b_o, drain diameter, and drain spacing, L; the complicated relationship is given by Bear (1972, p. 412) and graphed by Bouwer (1978, p. 296). The maximum rise of the water table, $M = h_1 - b_o$. Once again approximating the average water table depth above the impermeable layer by $D1 = 2h_1 - b_o$, equation X-29 can be manipulated to

$$\begin{aligned} f &= \left[\left(h_1 - b_o\right)^2 + 2D_e\left(h_1 - b_o\right)\right] 4K/L^2 = \\ &= \left[\left(D1 - b_o\right)^2 + D_e D1 - D_e b_o\right] 16K/L^2 \end{aligned} \tag{X-30}$$

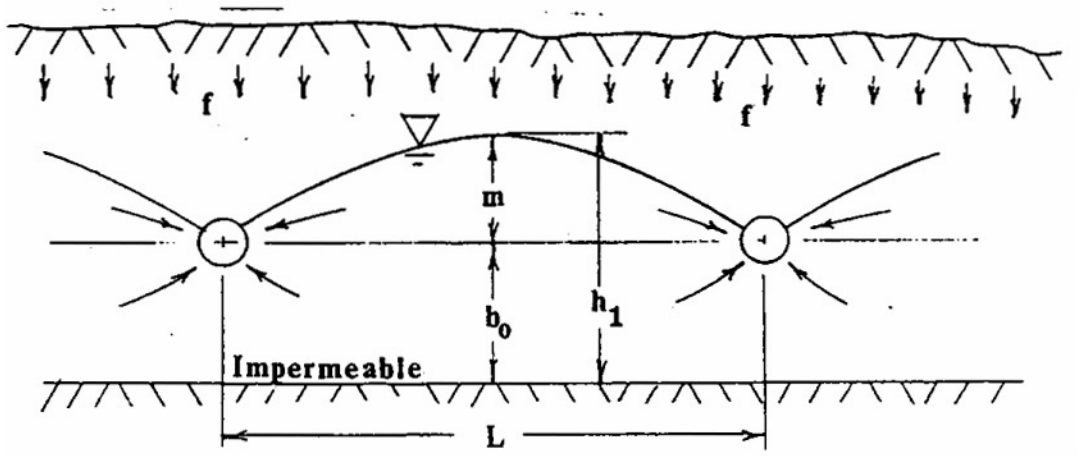

Figure X-9. Definition sketch for Hooghoudt's method for flow to circular drains.

Comparing equation X-30 with equations X-24 and X-25 yields

$A1 = 16K/L^2$,

$B1 = 2$

$A2 = 16KD_e b_o/L^2$

$B2 = 0$

$A3 = 16KD_e/TW\ L^2$

and $TW = BC = b_o$ = constant during the simulation. The equivalent depth, D_e, must be obtained from the sources indicated above. The mathematics of drainage to ditches or circular drains is complex» several alternative formulations are described by van Schilfgaarde (1974).

Limitations

Since the moisture content of the unsaturated zone is taken as an average over the entire zone, the shape of the moisture profile is totally obscured. Therefore, infiltrated water cannot be modeled as a diffusing slug moving down the unsaturated zone, as is the case in the real system. Furthermore, water from the capillary fringe of the saturated zone cannot move upward by diffusion or "suction" into the unsaturated zone.

The simplistic representation of subsurface storage by one unsaturated "tank" and one saturated "tank" limits the ability of the user to match non-uniform soil columns. Another limitation is the assumption that the infiltrated water is spread uniformly over the entire catchment area, not just over the pervious area. In addition, just as for surface flow, groundwater may not be routed from one subcatchment to another. The tendency of the tailwater influence to cause pulses if TW-BC is equated to the dynamic water depth in the adjacent channel is a limitation that will remain until the channel flow and subsurface flow are solved simultaneously using a set of coupled equations. Such a solution would also permit reverse flow or recharge from the channel to be simulated.

Finally, water quality is not simulated in any of the subsurface routines. If water quality is simulated in RUNOFF and the subsurface flow routines activated, any loads entering the soil will "disappear," as if the soil provides 100 percent treatment.

Subroutine Configuration

A flowchart of the subroutine configuration is presented in Figure X-10. Initial values and constants used in subroutine GROUND come mostly from subroutine GRIN, designed specifically to read in these values. Subroutine GRIN is called by RHYDRO. Other necessary values are transferred during the CALL statement and from previously calculated values stored in COMMON.

Subroutine GROUND first initializes pertinent parameters, then calculates fluxes that are constant over the time step. Beginning-of-time-step fluxes are calculated next, and the value of percolation is checked to ensure that it will not raise the water table above the ground surface.

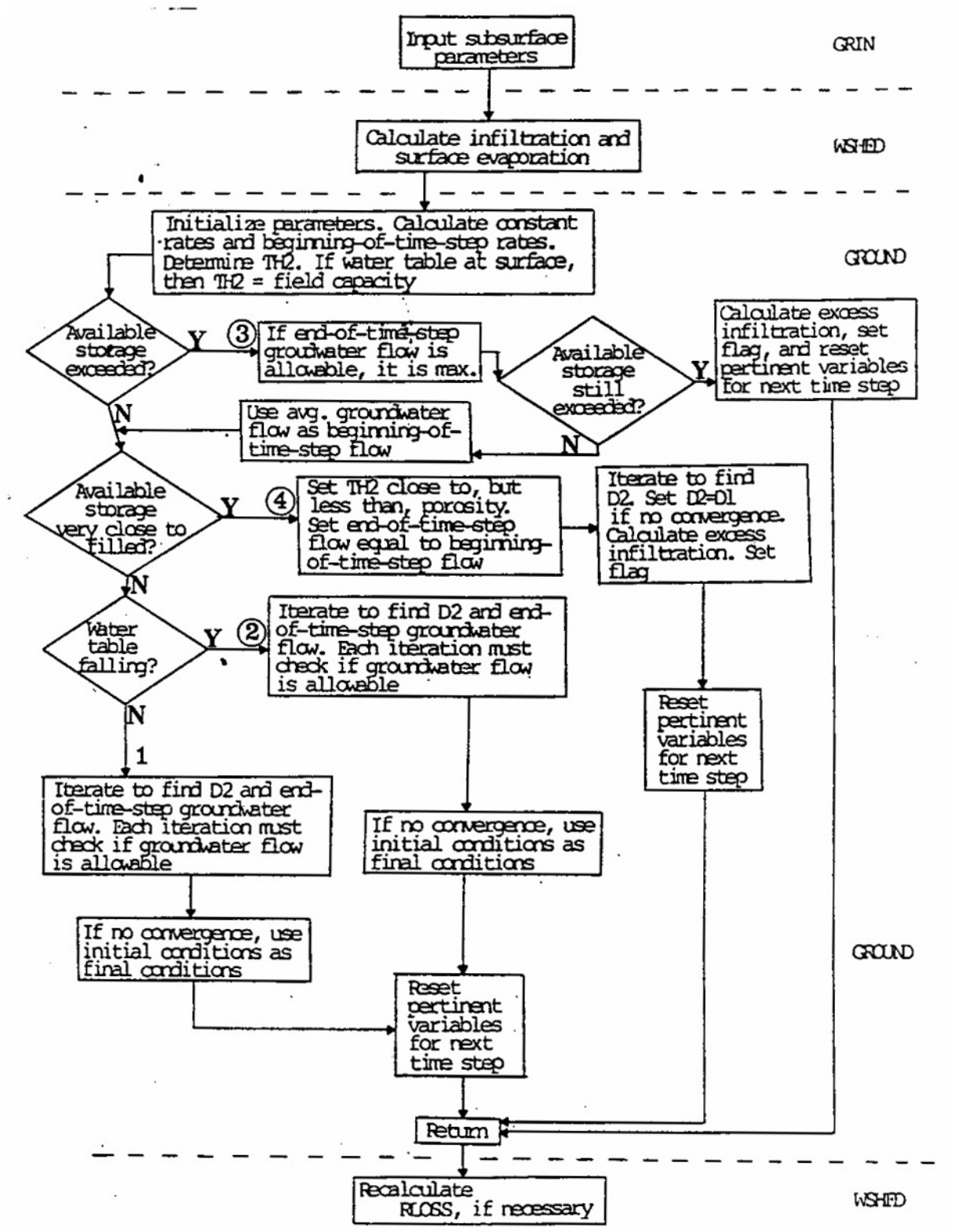

Figure X-10. Flowchart of subsurface and directly connected surface calculations.

After other constants are calculated and TH^2 is determined from equation X-4, the program branches to one of four areas. The first and second areas are for rising and falling water tables, equations X-2 and X-3, respectively. In both cases, Newton-Raphson iteration is used to solve simultaneously for the final groundwater flow, depth of lower zone, and deep percolation. Each iteration checks whether or not groundwater flow is possible (D1 greater than or equal to TW and BC). After the iterations converge, final conditions are set as the next time step's initial conditions.

In the event of saturation (D1 = DTOT), the third area sets D2 equal to DTOT, sets final ground-water flow equal to the maximum possible (D2 = DTOT), and assumes DEPPRC remains constant over the time step. Any excess infiltration is then routed back to the surface for overland flow calculations, and final conditions are set for the next initial conditions. However, if the maximum groundwater flow and DEPPRC rates permit some infiltration into the subsurface zone, the initial and final groundwater flow are averaged to be used as the new initial ground-water flow, and the program branches back to iterate for the solution. This pathway will rarely, if ever, be taken, but must be included to minimize possible continuity errors.

In the event the available storage in the unsaturated zone is less than 0.0001 ft, the fourth area sets TH2 equal to 90% of porosity and D2 close to DTOT, and returns any infiltration to the surface that causes the final unfilled upper zone volume to be greater than 0.0001 ft. This is to avoid oscillations as the water table hovers near the ground surface. Again, final conditions are then set as the next time step's initial conditions.

Examples

Cypress Creek Calibration and Verification

Two examples will illustrate the use of the new subroutine. The first example is a year-long simulation of a 47 mi^2 portion of the 117 mi^2 Cypress Creek Watershed in Pasco County, Florida, about 30 miles north of Tampa (Figure X-11). The region has been studied in relation to the interaction of surface water and ground water under the stress of heavy pumping and drainage activities in the area (Heaney et al., 1986). The watershed is characterized by sandy soils in which most water movement follows subsurface pathways. For this example, only a single 47 mi^2 area above State Road 52 (Figure X-11) and tributary to the USGS gage at San Antonio has been simulated.

Twenty-four parameters on three additional H-cards are required for each subsurface subcatchment. (Many of these can be ignored or set to zero during most runs» not all parameters are required for all runs.) Input parameters are echoed on two new pages of output that immediately follow the surface subcatchment information. Figure X-12 is an example of these two new pages; the values in Figure X-12 are from the calibration run on Cypress Creek. In addition to the new output just mentioned, a subsurface continuity check is provided in addition to the existing surface continuity check. An example of this amended page is shown in Figure X-13.

The simulation is divided into two six-month runs: the first six months for calibration, and the second six months for verification. Since Cypress Creek is a very flat, pervious area with well-drained soils and very little surface flow, it was modeled in a manner that would allow groundwater flow to account for most of the flow in the channel. In other words, the groundwater parameters represented by far the most critical part of the calibration. The only complete rainfall data for the calibration period are for the gage at St. Leo, out of the catchment to the east. Although these data are in daily increments, the calibration process was relatively

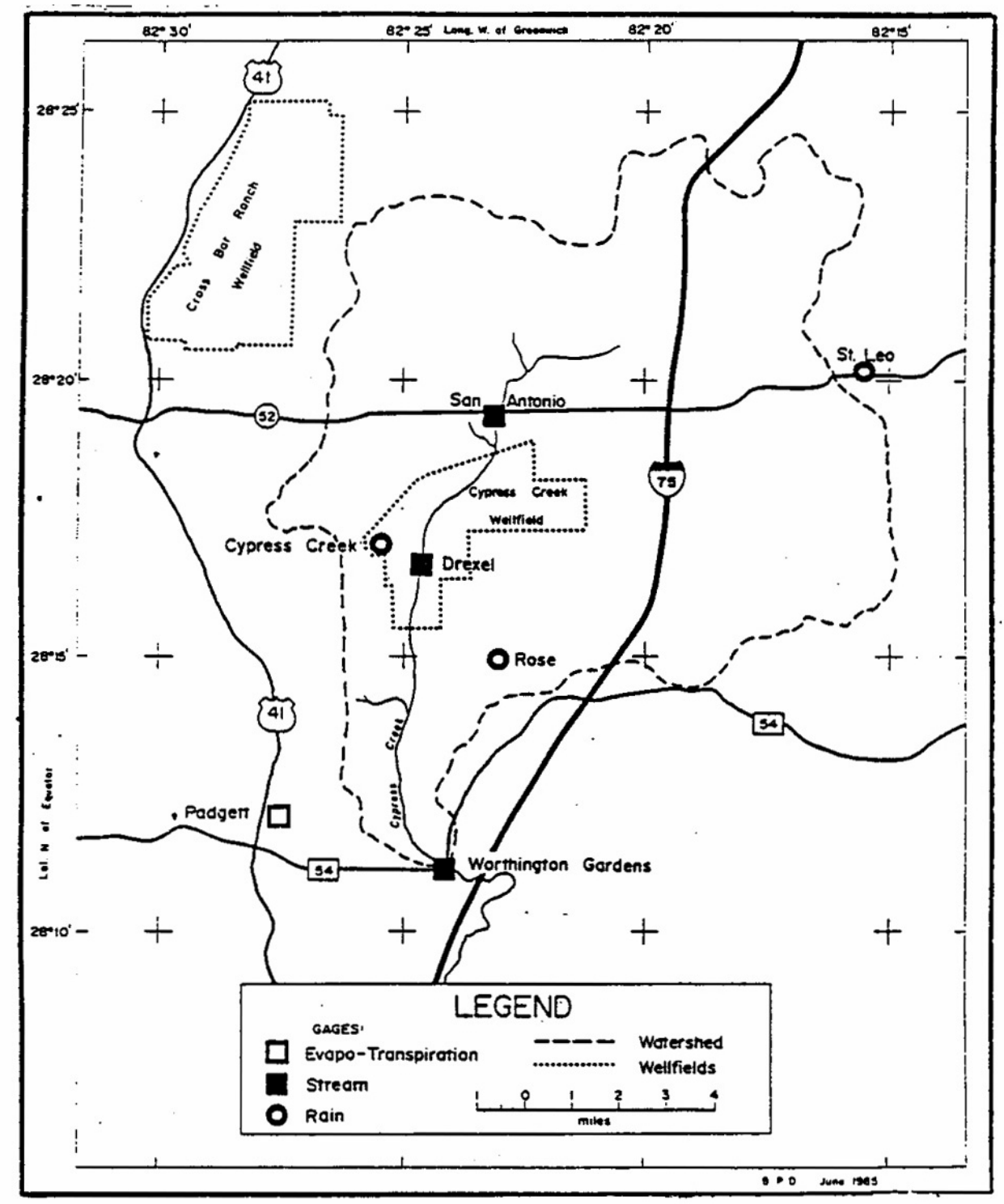

Figure X-11. Map of Cypress Creek watershed in Pasco County, Florida (Heaney et al., 1986).

* * * * * GROUNDWATER INPUT DATA * * * * * *

SUBCAT. NO.	GUTTER OR INLET	ELEVATIONS GROUND (FT)	BOTTOM (FT)	INITIAL STAGE (FT)	BC (FT)	TW (FT)	FLOW CONSTANTS A1 (IN/HR-FT**B1)	B1	A2 (IN/HR-FT**B2)	B2
21	22	20.00	0.00	7.20	8.55	8.55	4.500E-05	2.600	0.000E+00	1.000

* * * * * GROUNDWATER INPUT DATA (CONTINUED) * * * * * *

SUBCAT. NO.	SOIL PROPERTIES POROSITY	SATURATED HYDRAULIC CONDUCTIVITY (IN/HR)	WILTING POINT	FIELD CAPACITY	INITIAL MOISTURE	MAX. DEEP PERCOLATION (IN/HR)	PERCOLATION PARAMETERS HCO *	PCO ** (FT)	ET PARAMETERS DEPTH OF ET (FT)	FRACTION OF ET TO UPPER ZONE
21	.4600	5.000	.1500	.3000	.3010	2.000E-03	10.00	15.00	14.00	0.350

HYD. CONDUCTIVITY = SAT. HYD. COND. * EXP((UPPER Z MOISTURE CONTENT - POROSITY) * HCO)
* PERCOLATION RATE = HYD. COND. * (1 + PCO * (UPPER ZONE MOISTURE CONTENT - FIELD CAPACITY)/(UPPER ZONE DEPTH/2))

Figure X-12. Subsurface input data for Cypress Creek calibration.

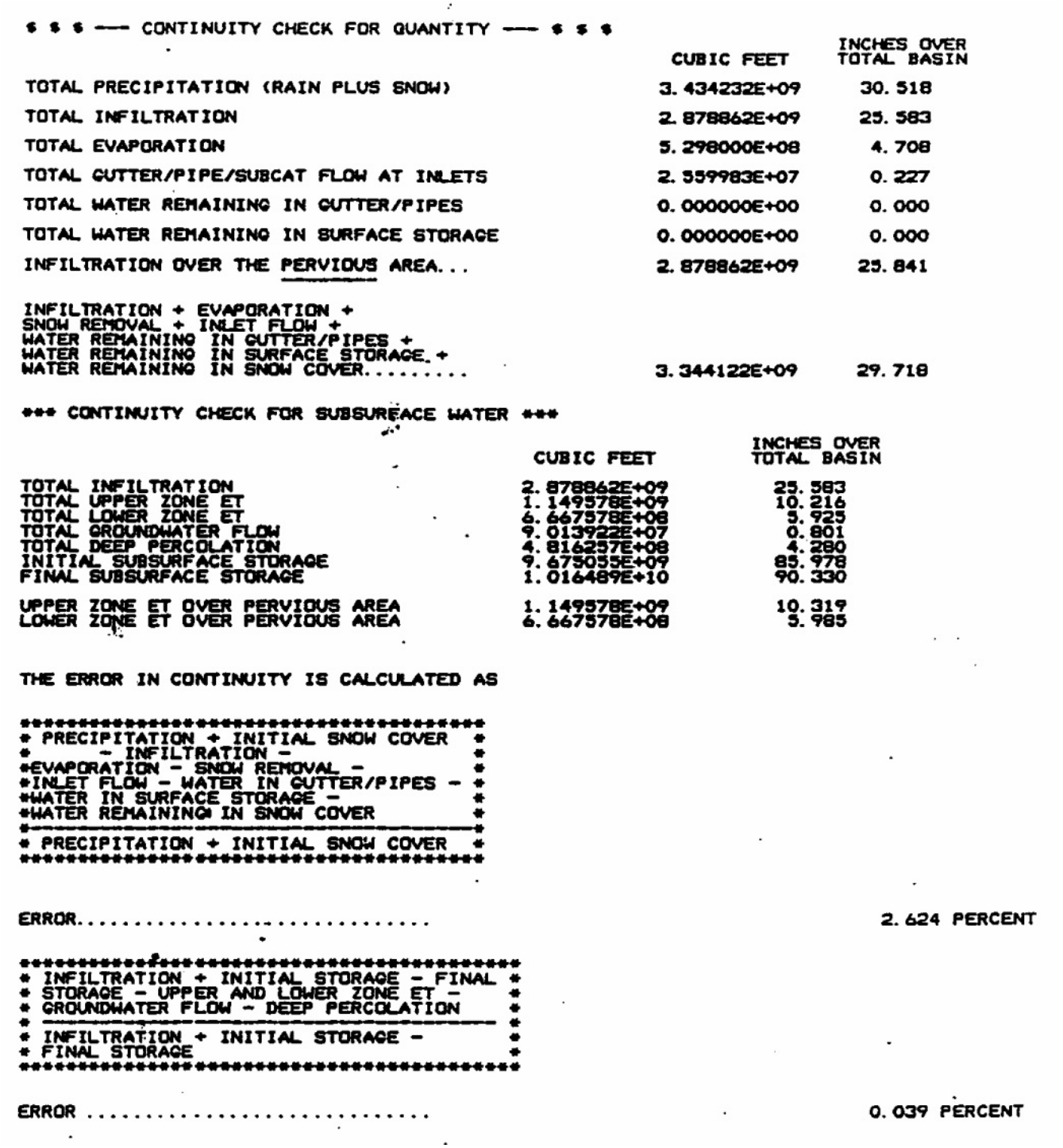

```
* * * ---- CONTINUITY CHECK FOR QUANTITY ---- * * *

                                                    CUBIC FEET    INCHES OVER TOTAL BASIN
TOTAL PRECIPITATION (RAIN PLUS SNOW)                3.434232E+09      30.518
TOTAL INFILTRATION                                  2.878862E+09      25.583
TOTAL EVAPORATION                                   5.298000E+08       4.708
TOTAL GUTTER/PIPE/SUBCAT FLOW AT INLETS             2.559983E+07       0.227
TOTAL WATER REMAINING IN GUTTER/PIPES               0.000000E+00       0.000
TOTAL WATER REMAINING IN SURFACE STORAGE            0.000000E+00       0.000
INFILTRATION OVER THE PERVIOUS AREA...              2.878862E+09      25.841

INFILTRATION + EVAPORATION +
SNOW REMOVAL + INLET FLOW +
WATER REMAINING IN GUTTER/PIPES +
WATER REMAINING IN SURFACE STORAGE +
WATER REMAINING IN SNOW COVER.....                  3.344122E+09      29.718

*** CONTINUITY CHECK FOR SUBSURFACE WATER ***

                                                    CUBIC FEET    INCHES OVER TOTAL BASIN
TOTAL INFILTRATION                                  2.878862E+09      25.583
TOTAL UPPER ZONE ET                                 1.149578E+09      10.216
TOTAL LOWER ZONE ET                                 6.667578E+08       5.925
TOTAL GROUNDWATER FLOW                              9.013922E+07       0.801
TOTAL DEEP PERCOLATION                              4.816257E+08       4.280
INITIAL SUBSURFACE STORAGE                          9.675055E+09      85.978
FINAL SUBSURFACE STORAGE                            1.016489E+10      90.330

UPPER ZONE ET OVER PERVIOUS AREA                    1.149578E+09      10.319
LOWER ZONE ET OVER PERVIOUS AREA                    6.667578E+08       5.985

THE ERROR IN CONTINUITY IS CALCULATED AS

*****************************************
* PRECIPITATION + INITIAL SNOW COVER    *
*       - INFILTRATION -                *
*EVAPORATION - SNOW REMOVAL -           *
*INLET FLOW - WATER IN GUTTER/PIPES -    *
*WATER IN SURFACE STORAGE -              *
*WATER REMAINING IN SNOW COVER          *
*---------------------------------------*
* PRECIPITATION + INITIAL SNOW COVER    *
*****************************************

ERROR.....                                          2.624 PERCENT

*****************************************
* INFILTRATION + INITIAL STORAGE - FINAL *
* STORAGE - UPPER AND LOWER ZONE ET -    *
* GROUNDWATER FLOW - DEEP PERCOLATION    *
* ---------------------------------------*
* INFILTRATION + INITIAL STORAGE -       *
* FINAL STORAGE                          *
*****************************************

ERROR .....                                         0.039 PERCENT
```

Figure X-13. Continuity check for surface and subsurface for Cypress Creek calibration. The relatively large surface continuity error does not actually exist; it comes from a double accounting of the groundwater flow – a problem that has been fixed.

simple because of the existence of both flow and shallow-well stage data. In addition, only one subcatchment (surface and subsurface) was used, since the purpose of this example was only to illustrate the use of subroutine GROUND, not to provide a thorough simulation.

Figure X-14 shows the predicted groundwater flow hydrograph and the measured total flow hydrograph for the calibration run, and Figure X-15 shows a comparison of the predicted total flow hydrograph to the measured total flow hydrograph for the calibration run. Predicted and measured stages for the calibration can be seen in Figure X-16. The calibration is not especially remarkable in light of the lack of detailed rainfall data for the 47 mi^2 area. The predicted stage hydrograph does not exhibit the short-term variations that are measured, primarily because of the lack of spatial detail in the rain. In addition, the measured stages are at one well near the center of the modeled area and would be expected to show more variation than would the average water table over the 47 mi^2 simulated by SWMM. The existence of more than one gage in the 47 square miles of the catchment and shorter increment rainfall data would have improved the fit seen in Figure X-16. Figures X-17, X-18 and X-19 show similar results for the verification runs. In general, the average recession of the water table is simulated accurately, but not the fluctuations.

Hypothetical Catchment with High Water Table

The second example is a 100 ac hypothetical subcatchment with the same soil properties as Cypress Creek and a water table that is initially one foot from the surface. The 10-yr SCS Type II design storm for Tallahassee, Florida, is used for the rainfall input (Figure X-20). This storm is characterized by very high rainfall between hours 11 and 12.

In order to illustrate the influence of a high water table, runs were made with and without the groundwater subroutine. Table X-2 shows the disposition of the rainfall when a high water table is simulated as opposed to when it is ignored. Note that evaporation is about the same, and the difference in the amount of infiltrated water shows up as a direct difference in surface runoff. (The runs were halted before all water had run off.) The two hydrographs and the corresponding water table (for the run in which it is simulated) are shown in Figure X-21. A larger difference in peak flows would have resulted if the flows had not been routed to a very large channel. Also, note that the two hydrographs are identical until about hour eleven into the simulation, when the simulated water table rises to the surface.

Execution time on the IBM 3033 mainframe increased from 0.32 CPU seconds without the groundwater simulation to 0.42 CPU seconds with the groundwater simulation. Thus, some additional computational expense can be expected.

Conclusions

Although the subroutine is fairly simple in design and has several limitations, the new groundwater subroutine should increase the applicability of SWMM. Preliminary test runs have determined it to be accurate in the simulation of water table stage and groundwater flow. Further calibration and verification tests need to be done on other areas to confirm these preliminary results. Also, estimation of parameters, although fairly numerous, appears to be relatively uncomplicated. In addition, parameters are physically based and should be able to be estimated from soils data. The flexible structure of the algorithm should permit a more realistic simulation of catchments in which a major hydrograph component is via subsurface pathways.

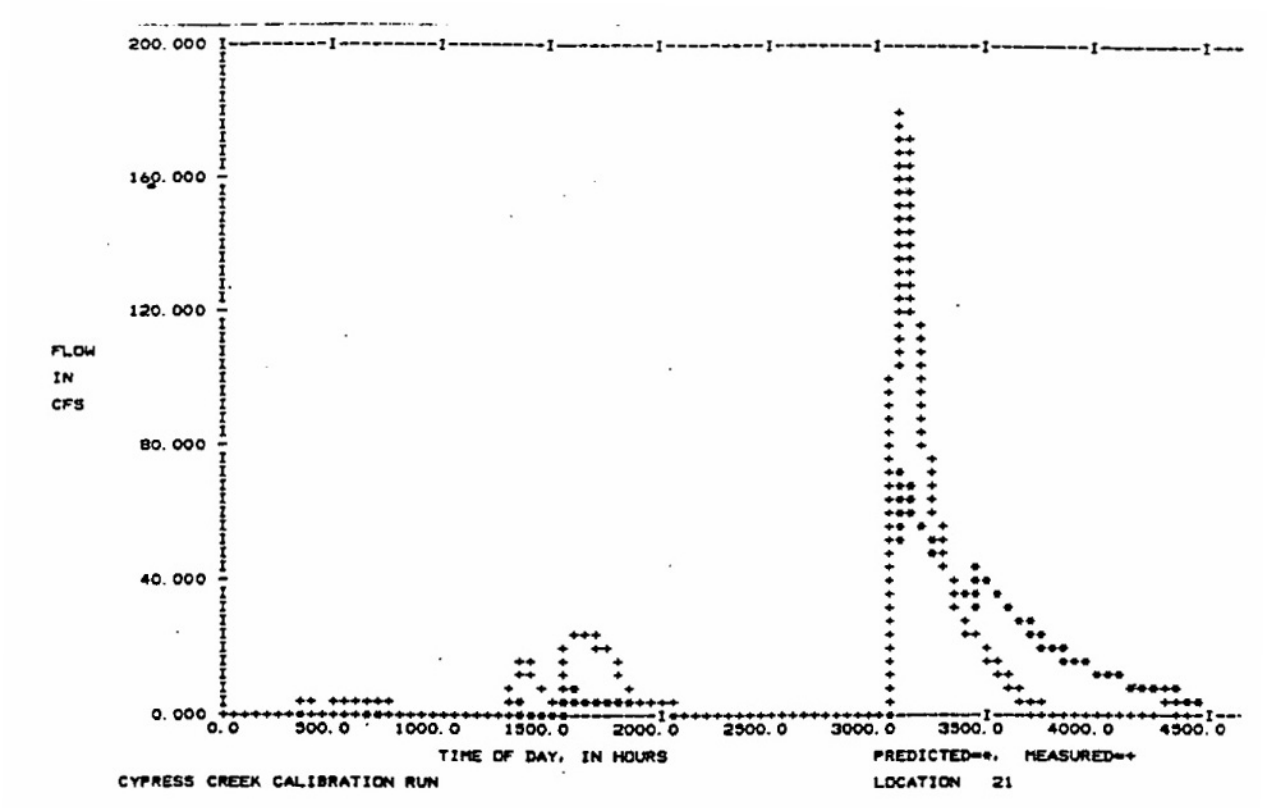

HYDROGRAPH STATISTICS FOR LOCATION 21

	VOLUME		PEAK FLOW		DURATION			NO.
	CUBIC FEET	INCHES	TIME, HR	FLOW, CFS	START, HR	END, HR	LENGTH, HR	POINTS
PREDICTED, TOTAL TIME	0.14547E+09	1.293	3105.000	73.242	0.000	4430.000	4430.000	194
MEASURED, TOTAL TIME	0.16359E+09	1.454	3120.000	180.000	0.000	4392.000	4392.000	184
PREDICTED, OVERLAPPING TIME	0.14463E+09	1.285	3105.000	73.242	0.000	4393.000	4393.000	192
MEASURED, OVERLAPPING TIME	0.16359E+09	1.454	3120.000	180.000	0.000	4392.000	4392.000	18
DIFFERENCES, ABSOLUTE	0.18964E+08	0.169	15.000	106.758				
% OF MEAS		11.592		59.310				

Figure X-14. Predicted groundwater flow hydrograph and total measured flow hydrograph for Cypress Creek calibration.

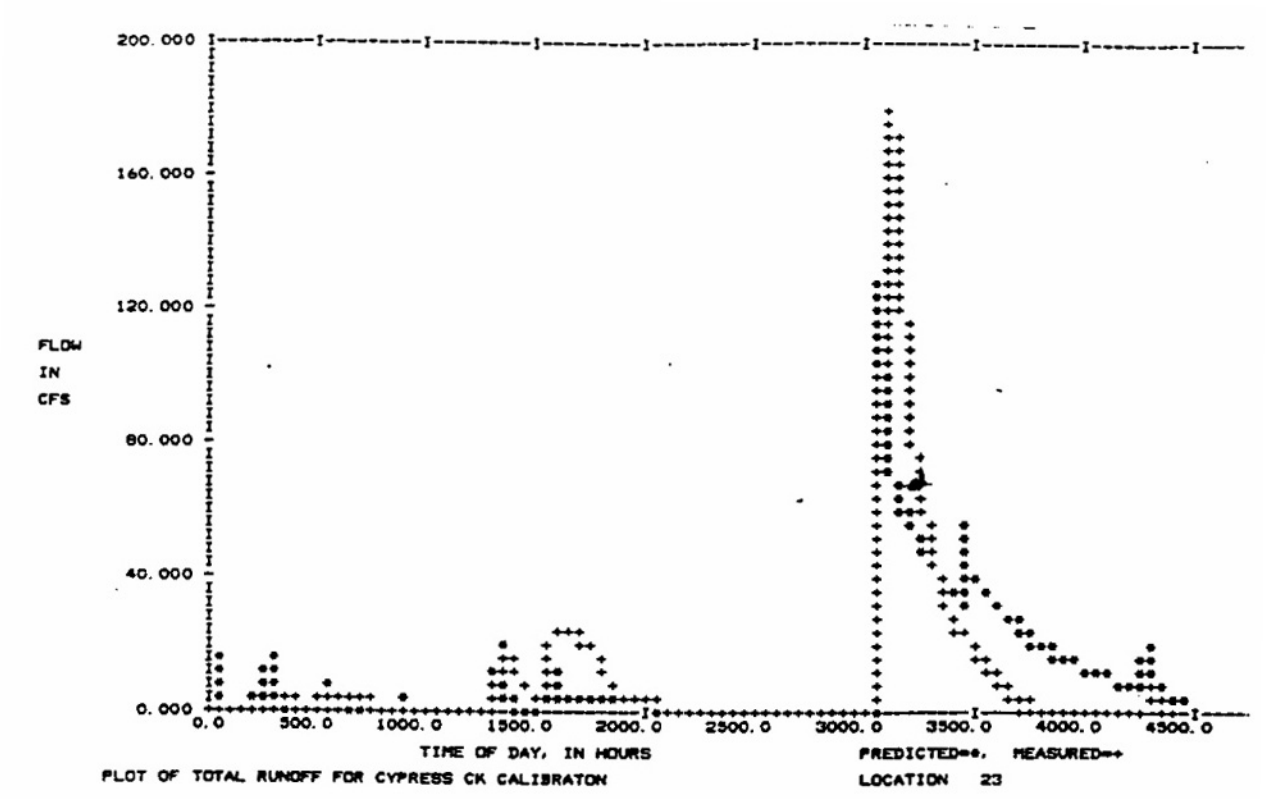

HYDROGRAPH STATISTICS FOR LOCATION 23

	VOLUME CUBIC FEET	VOLUME INCHES	PEAK FLOW TIME, HR	PEAK FLOW FLOW, CFS	DURATION START, HR	DURATION END, HR	DURATION LENGTH, HR	NO. POINTS
PREDICTED. TOTAL TIME	0.17127E+09	1.522	3059.000	128.228	0.000	4430.000	4430.000	194
MEASURED. TOTAL TIME	0.16359E+09	1.454	3120.000	180.000	0.000	4392.000	4392.000	184
PREDICTED. OVERLAPPING TIME	0.17042E+09	1.514	3059.000	128.228	0.000	4393.000	4393.000	192
MEASURED. OVERLAPPING TIME	0.16359E+09	1.454	3120.000	180.000	0.000	4392.000	4392.000	184
DIFFERENCES. ABSOLUTE	-0.68276E+07	-0.061	61.000	51.772				
% OF MEAS		-4.174		28.762				

Figure X-15. Total predicted flow hydrograph and total measured flow for Cypress Creek calibration.

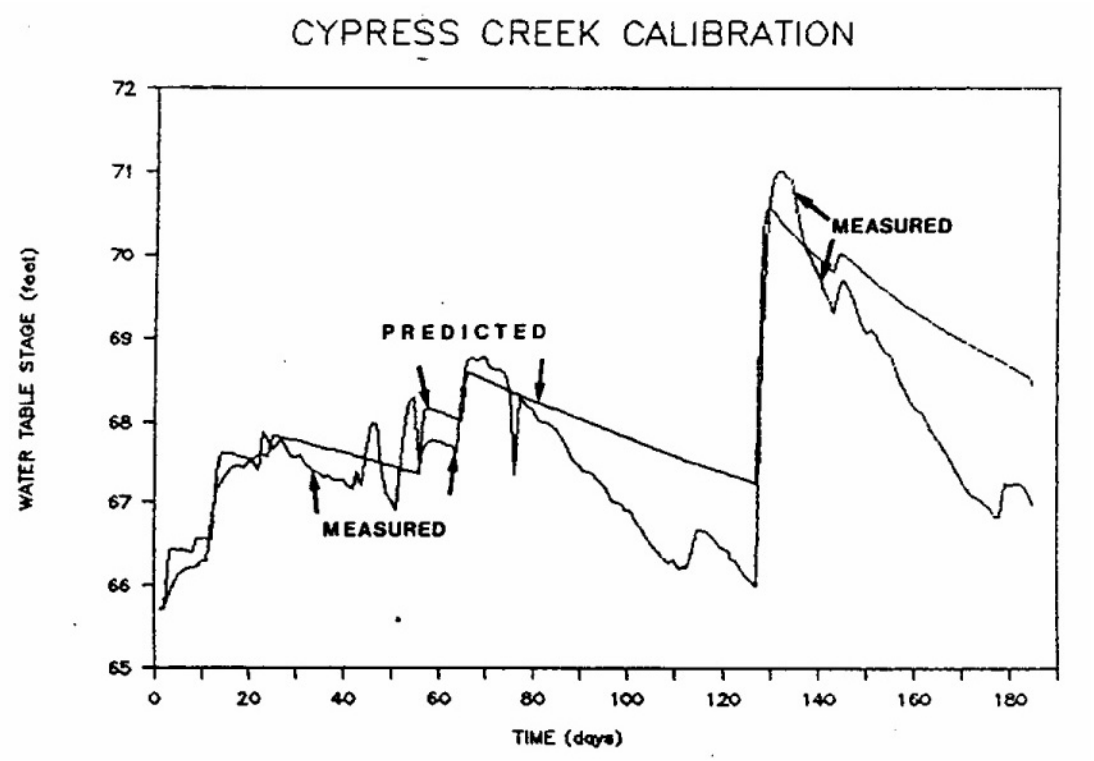

Figure X-16. Predicted and measured stages for Cypress Creek calibration.

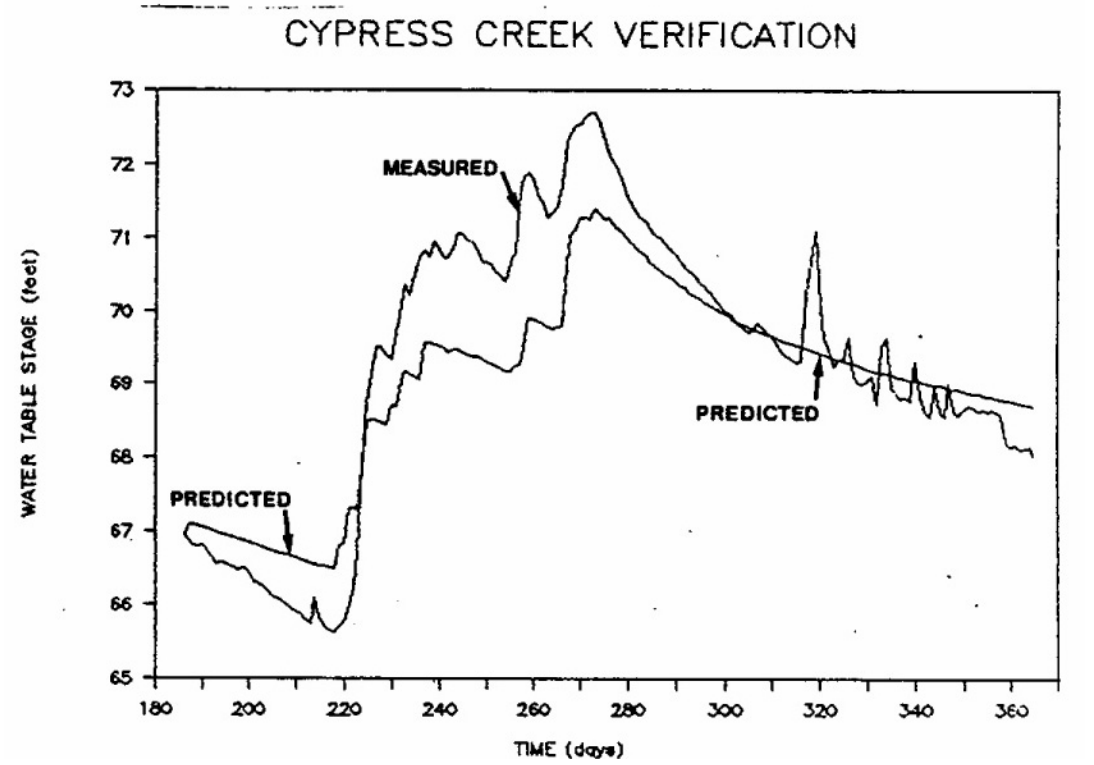

Figure X-17. Predicted and measured stages for Cypress Creek calibration.

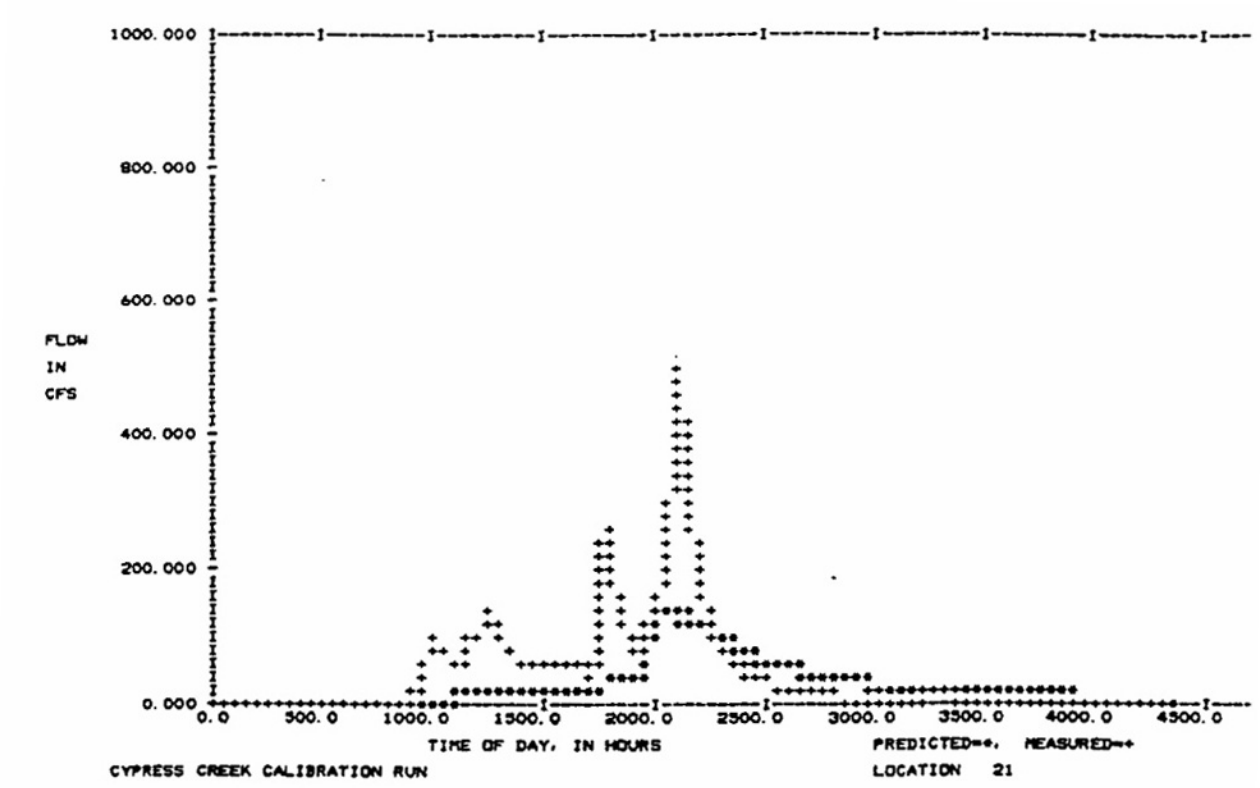

HYDROGRAPH STATISTICS FOR LOCATION 21

	VOLUME		PEAK FLOW		DURATION			NO.
	CUBIC FEET	INCHES	TIME, HR	FLOW, CFS	START, HR	END, HR	LENGTH, HR	POINTS
PREDICTED, TOTAL TIME	0.42533E+09	3.780	2112.000	144.583	0.000	4350.000	4350.000	199
MEASURED, TOTAL TIME	0.71232E+09	6.330	2112.000	500.000	0.000	4320.000	4320.000	181
PREDICTED, OVERLAPPING TIME	0.42426E+09	3.770	2112.000	144.583	0.000	4312.000	4312.000	197
MEASURED, OVERLAPPING TIME	0.71232E+09	6.330	2112.000	500.000	0.000	4320.000	4320.000	181
DIFFERENCES, ABSOLUTE	0.28806E+09	2.560	0.000	355.417				
% OF MEAS		40.440		71.083				

Figure X-18. Predicted groundwater flow hydrograph and total measured flow hydrograph for Cypress Creek verification.

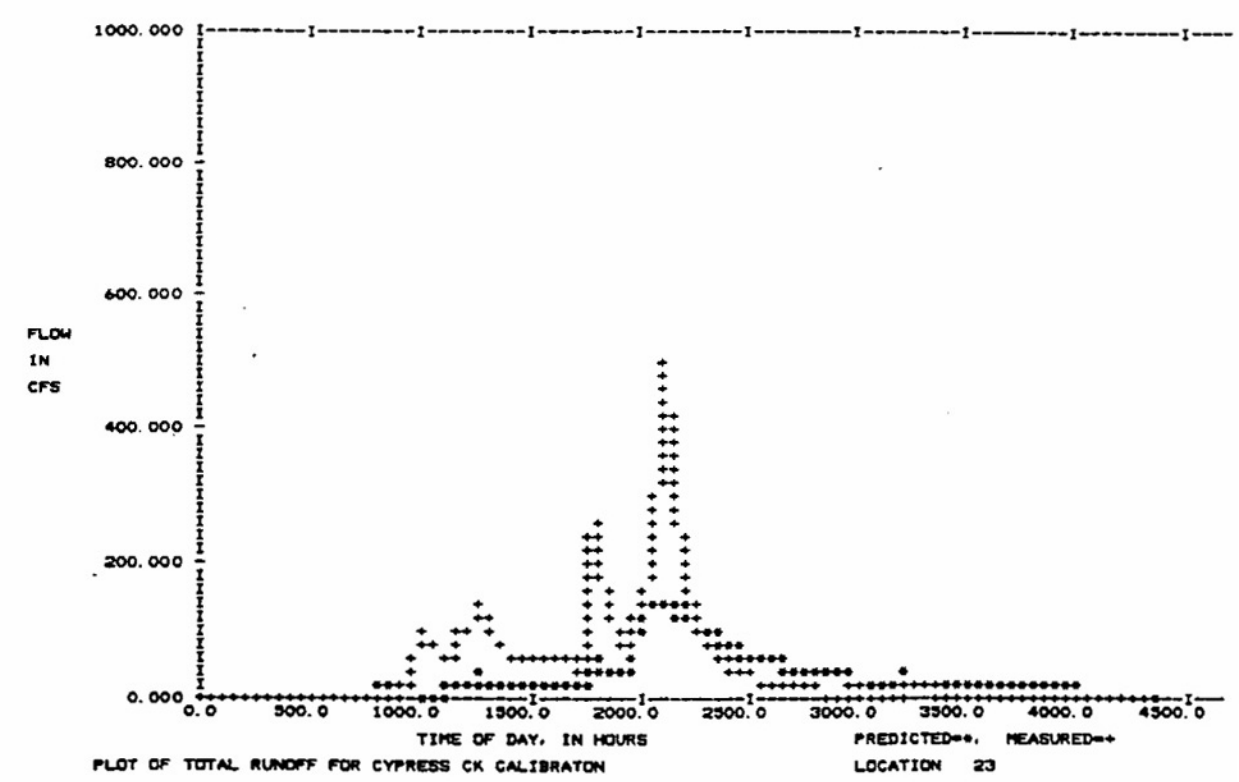

HYDROGRAPH STATISTICS FOR LOCATION 23

	VOLUME		PEAK FLOW		DURATION			NO.
	CUBIC FEET	INCHES	TIME, HR	FLOW, CFS	START, HR	END, HR	LENGTH, HR	POINTS
PREDICTED, TOTAL TIME	0.44397E+09	3.945	2112.000	149.908	0.000	4350.000	4350.000	199
MEASURED, TOTAL TIME	0.71232E+09	6.330	2112.000	500.000	0.000	4320.000	4320.000	181
PREDICTED, OVERLAPPING TIME	0.44289E+09	3.936	2112.000	149.908	0.000	4312.000	4312.000	197
MEASURED, OVERLAPPING TIME	0.71232E+09	6.330	2112.000	500.000	0.000	4320.000	4320.000	181
DIFFERENCES, ABSOLUTE	0.26943E+09	2.394	0.000	350.092				
% OF MEAS		37.824		70.018				

Figure X-19. Total predicted flow hydrograph and total measured flow for Cypress Creek verification.

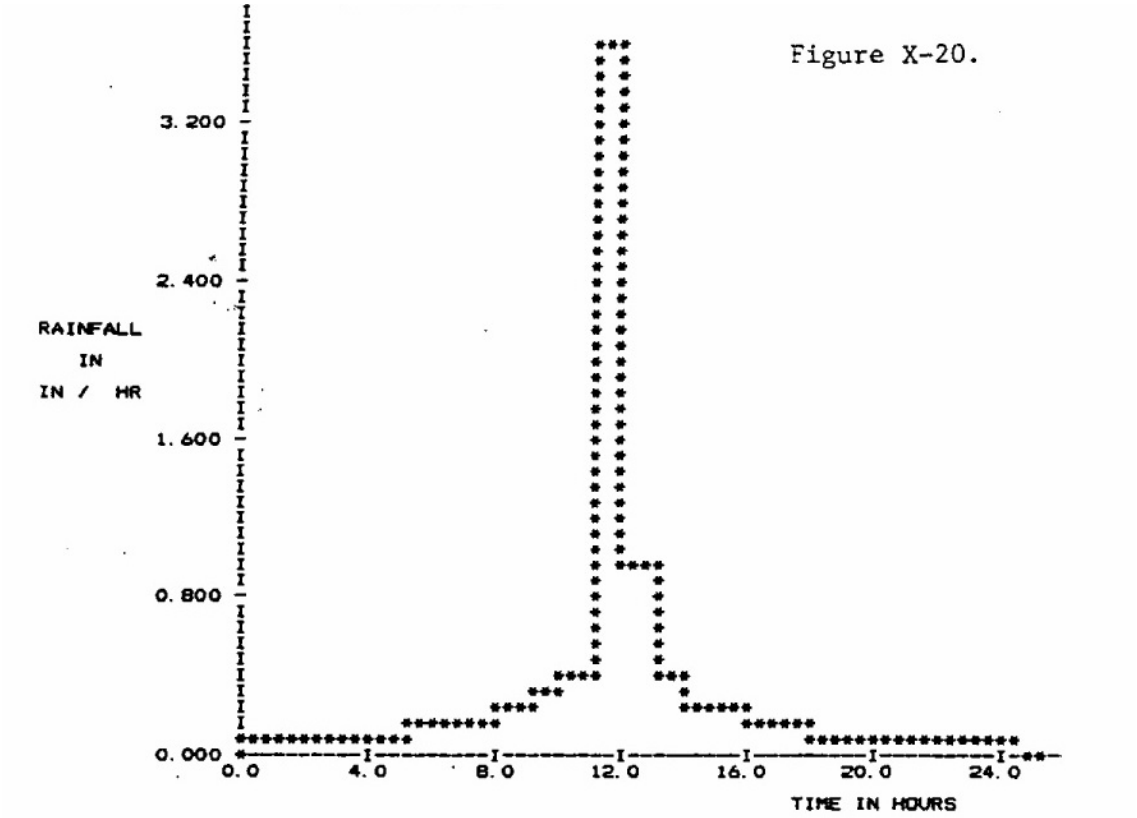

Figure X-20. Hydrograph for hypothetical subcatchment (10-yr SCS Type II design storm for Tallahassee, Florida).

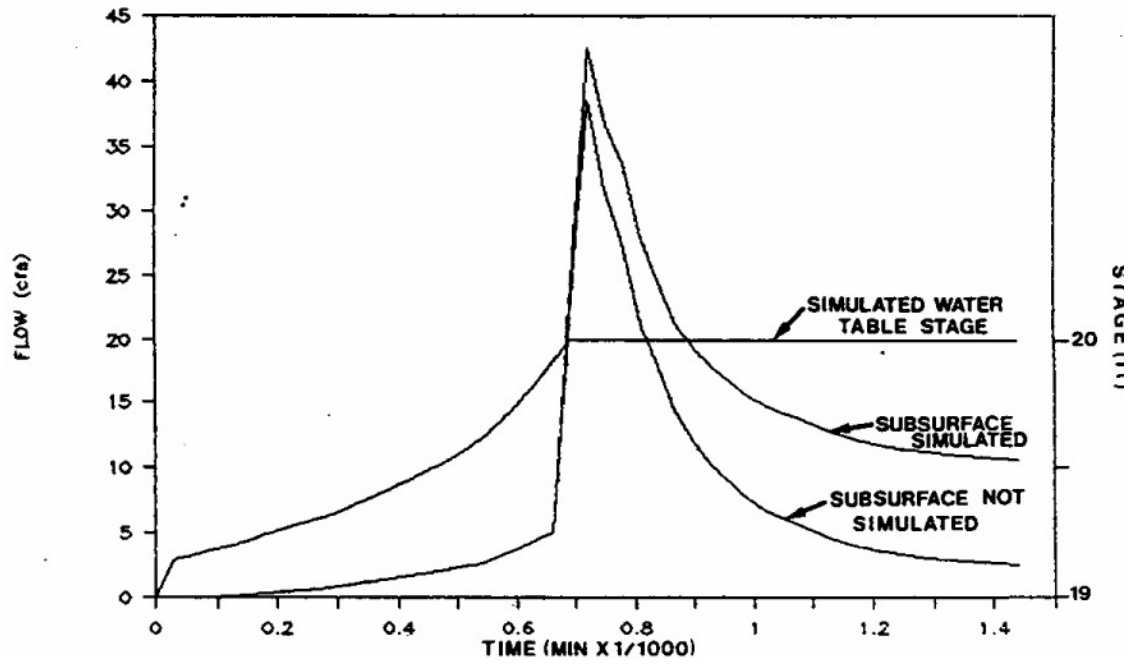

Figure X-21. Hydrographs of surface flow and simulated water table stage from hypothetical subcatchment. The hydrographs are identical until the water table reaches the surface (20 ft).

Table X-2. Fate of Runoff With and Without High Water Table Simulation

	Inches Over Total Basin	
Water Budget Component	With Water Table Simulation	Without Water Table Simulation
Precipitation	8.399	8.399
Infiltration	6.637	1.731
Evaporation	0.103	0.104
Channel flow at inlet	1.495	2.407
Water remaining in channel	0.015	0.038
Water remaining on surface	0.150	4.124
Continuity error	0.001	0.005